Interannual Variations of Summer Monsoons: Sensitivity to Cloud Radiative Forcing

O.P. Sharma, Hervé Letreut, Genevieve Seze, Laurent Fairhead, R. Sadourny

Interannual Variations of Summer Monsoons: Sensitivity to Cloud Radiative Forcing

O. P. SHARMA, H. LE TREUT, G. SÈZE, L. FAIRHEAD, AND R. SADOURNY

Laboratoire de Météorologie Dynamique, Ecole Normale Supérieure, Paris, France

(Manuscript received 25 April 1995, in final form 3 November 1997)

ABSTRACT

The sensitivity of the interannual variations of the summer monsoons to imposed cloudiness has been studied with a general circulation model using the initial conditions prepared from the European Centre for Medium-Range Forecasts analyses of 1 May 1987 and 1988. The cloud optical properties in this global model are calculated from prognostically computed cloud liquid water. The model successfully simulates the contrasting behavior of these two successive monsoons. However, when the optical properties of the observed clouds are specified in the model runs, the simulations show some degradation over India and its vicinity. The main cause of this degradation is the reduced land–sea temperature contrast resulting from the radiative effects of the observed clouds imposed in such simulations. It is argued that the high concentration of condensed water content of clouds over the Indian land areas will serve to limit heating of the land, thereby reducing the thermal contrast that gives rise to a weak Somali jet. A countermonsoon circulation is, therefore, simulated in the vector difference field of 850-hPa winds from the model runs with externally specified clouds. This countermonsoon circulation is associated with an equatorial heat source that is the response of the model to the radiative effects of the imposed clouds. Indeed, there are at least two clear points that can be made: 1) the cloud–SST patterns, together, affect the interannual variability; and 2) with both clouds and SST imposed, the model simulation is less sensitive to initial conditions. Additionally, the study emphasizes the importance of dynamically consistent clouds developing in response to the dynamical, thermal, and moist state of the atmosphere during model integrations.

1. Introduction

The ''vagaries of monsoon'' are well known to the people of the Indian subcontinent. In some years the monsoon is good, bringing more than normal rainfall to this region, while for some other years, the seasonal total of the rainfall remains well below normal, due to a bad monsoon. In order to understand the intriguing behavior of the monsoon phenomenon, several researchers have conducted both observational and modeling studies. From observational studies on rainfall, pressure, and wind fields, it is now a well-established fact that the summer monsoon over and around India exhibits variations both on intraseasonal and interannual timescales (Madden and Julian 1994). Modeling studies on monsoon variability have started ever since Charney and Shukla (1981) pointed out that a large part of low-latitude variability is due to boundary anomalies in such quantities such as sea surface temperature (SST), albedo, and soil moisture. Later, Shukla (1981) also argued that this low-frequency (seasonal) variability should be predictable from atmospheric general circulation models (GCMs). The slow evolution of these boundary forcings thus makes the prospect of atmospheric predictions achievable on seasonal timescales (Palmer et al. 1990).

The contrast monsoon years of 1987 and 1988 provide an excellent opportunity for modelers who are interested in studying the interannual variations of Northern Hemisphere summer monsoons with the help of atmospheric GCMs. Seasonal integrations of these models are required in order to assess how well they simulate the low-frequency variability of monsoon circulation. The GCMs are also used to test any hypothesis made on the interannual variability of the Indian monsoon (Chen and Yen 1994). Observational studies are utilized in evaluating the performance of atmospheric models in simulating such modes of oscillations. Regarding the summer monsoons of 1987 and 1988, the evolution of several important parameters, which are believed to be responsible for these two successive but contrasting monsoons, have been studied in detail by Krishnamurti et al. (1989, 1990). Their studies reveal that during 1987 the lower-tropospheric streamfunction anomaly showed pronounced countermonsoon circulation that was absent in 1988. Since moisture supply is important for good performance of monsoons, Krishnamurti et al. (1990) have pointed out that the warm SST anomaly over the Bay of Bengal contributed to the supply of moisture during the active monsoon season of 1988. It may be remarked that the seasonal (June–September) difference field of SST for 1988 and 1987 shows weak negative

Corresponding author address: Dr. O. P. Sharma, Centre for Atmospheric Sciences, Indian Institute of Technology, New Delhi 110016, India. E-mail: opsharma@henna.iitd.ernet.in

SST anomalies in the Arabian Sea and positive anomalies less than 0.5°C to the east. Also, SST anomalies are very irregular from month to month. The SST anomalies for September are found to be very important for the monsoon rainfall.

Another parameter, the velocity potential, showed major ascent over the monsoon region and descents over the Atlantic Ocean, the eastern Pacific Ocean, and North America, which is indicative of above-normal monsoon activity in 1988. But during 1987, the monsoonal divergent circulation was much smaller in extent with the center of divergence displaced far to the southeast of the Indian monsoon region. So most important differences between these two successive monsoons are seen in the streamfunction and velocity potential fields, which also provide an insight into the structure of large-scale atmospheric flow. While 1987 was a drought year of a major ENSO activity, above-normal rainfall occured during the summer of 1988 over most of the Indian subcontinent (Das et al. 1988; Das et al. 1989). However, it may be noted that 1988 was a drought year in the United States and tropical SST anomalies had a significant effect in reducing the precipitation in this region (Atlas et al. 1993).

In a recent study, Palmer et al. (1992) have reported their findings from a large number of 90-day numerical experiments performed with the T42 version of the forecasting model of the European Centre for Medium-Range Weather Forecasts (ECMWF) with the initial conditions of 1 June 1987 and 1988 and forced with a variety of SST datasets. The ECMWF model has successfully simulated the interannual variations both in streamfunction and velocity potential with prescribed initial and boundary conditions. On a regional basis, the rainfall over the Sahel and to some extent over India have shown correct sense of interannual variations, though the model appeared to have an overall dry bias. However, Palmer et al. have made an important observation on the basis of identical SSTs but different initial conditions: that a nonnegligible fraction of the variance of month-to-seasonal rainfall, particularly, over India may not be dynamically predictable. Moreover, it appears that the seasonal variability of monsoon rainfall also depends on the initial conditions in the GCMs. Another study (Sperber and Palmer 1996) evaluated the interannual variability of rainfall over the Indian subcontinent, African Sahel, and Nordeste region of Brazil in 32 models for the period 1979–88 as part of the Atmospheric Model Intercomparison Project (AMIP). The interannual variations of the Nordeste rainfall are readily simulated (because it is intimately linked with the Pacific and Atlantic SSTs), but the rainfall variations over India and Sahel were less well simulated. From an ensemble of six ECMWF AMIP runs, differing only in their initial conditions, Sperber and Palmer (1996) found that the model reproduced the contrasting behavior in all 1987 and 1988 in each of these realizations, but in other years the all-India rainfall variability showed little or no predictability, possibly due to the internal chaotic dynamics and/or the unpredictable land surface process interaction. Thus, there is a need to examine other factors too, for example, cloud forcing, that contribute to monsoon variability because SST is not the only factor that determines monsoon. When more forcing parameters are specified, whether the month-to-seasonal rainfall is still a function of the initial conditions is a topic of considerable interest, because it gives an idea of what the natural processes are that may interact to extend the predictability of the monsoon system.

Most of the simulations presented so far have been achieved mainly from model integrations (WCRP 1992, 1993) that have been forced by observed SSTs. Such simulations of the Indian summer monsoon have been performed in order to achieve the objectives of the Monsoon Numerical Experimentation Group. Additional sensitivity experiments are necessary to sort out the physical processes that explain the model response. In particular, numerical experiments may be performed with forcings not only at the earth–atmosphere interface but also that arise due to clouds. Indeed, the specification of SSTs in sensitivity experiments is a tried and true technique because such experiments test the response of the model to the imposition of an external condition (or boundary forcing). However, clouds arise in a model (and the atmosphere, for that matter) as a consequence of complex interactions between internal thermodynamical and dynamical processes. When the model produces its own clouds, such cloud features are internally consistent with model dynamics and thermodynamics that are part and parcel of the model simulation. In some models, like the one used here for the present study, cloud parameters are computed from a prognostic state variable, the cloud liquid water content (LWC). Since some of the cloud parameters can now be derived from the well-documented satellite datasets, one can use them directly in GCM experiments. However, when clouds are imposed in this manner, they may not be consistent with the model dynamics and thermodynamics giving rise to spurious heat sources, heating rates, radiative anomalies, etc., that, in turn, cause a cascade of errors in the GCM simulation. Therefore, it is of considerable interest to know how the model responds to the radiative forcing resulting from the specification of clouds and their properties from the satellite data. The imposition of clouds externally in a simulation run amounts to changes in cloud parameters, hence their impact can also be evaluated through sensitivity experiments. In some of the simulation runs the International Satellite Cloud Climatology Project (ISCCP) clouds were imposed because they are as close to observations as possible.

The ISCCP was established in 1982 as the first project of the World Climate Research Program (WCRP) to produce a new cloud climatology over the whole globe. The analyses of ISCCP provide globally uniform information on cloud feedback parameters. For this study, the ISCCP C1 analyses (Rossow and Schiffer 1991) for

four months (May–August) of 1987 and 1988 have been utilized to derive the pertinent parameters. The important features of ISCCP C1 datasets are 1) they represent a detailed description of the global distribution of cloud amount with a resolution of 280 km, 2) they provide variations of cloud amount on timescales from 3 h to several years, and 3) they provide a relatively uniform coverage of the whole globe. An interesting comparison of ISCCP and other cloud amounts has been reported recently by Rossow et al. (1993).

The diabatic heat sources and sinks play an important role in the shaping of the tropical climate. It is known that latent heat release in clouds constitutes an important heat source in the Tropics. The dynamics of the tropical atmosphere is also controlled both by local and remotely situated heat sources in the low latitudes. Gill (1980) elucidated the response of the tropical atmosphere to diabatic heat sources using a simple analytical model. He pointed out that a symmetric heat source over the equator produces, in the lower troposphere, easterly flow (Kelvin response) to the east and strong westerly inflow (Rossby response) to the west of the source region. But when the heating is displaced north of the equator, flow similar to the monsoon circulation of July is produced. This important study has thus emphasized the role of heat sources in the tropical atmosphere and particularly its response to their location and distribution about the equator. Further studies with the help of an axisymmetric model (Lindzen and Hou 1988; Hou and Lindzen 1992) showed that the strength of the Hadley circulation depends on the location of heat sources. Moreover, even small changes in the distribution of tropical heating can profoundly change the intensity of the Hadley circulation and the baroclinicity in the extratropics. These studies, without feedback between forcing and circulation, nevertheless show the sensitivity of the zonally averaged low-latitude circulation to displacement of heating from the equator. In a recent study, Zhang and Krishnamurti (1996) obtained the generalized Gill's solutions in the entire tropical belt to describe the response of the tropical circulation to the global tropical heat sources and sinks retrieved from satellite-based field of outgoing longwave radiation. These solutions exhibit most of the climatological features of the wintertime and the summertime (including the Asian monsoon) circulations of the lower troposphere. The Asian summer monsoon arises due the land–sea temperature contrast, which is influenced by external conditions and internal feedbacks (Meehl 1994a,b). The strength of the monsoon increases (decreases) as this contrast increases (decreases). It has been illustrated and suggested by Meehl (1994a) that external conditions involving land albedos (Charney et al. 1977) could reduce the land–sea temperature contrast leading to a weak monsoon, while internal feedback could increase it leading to a good monsoon. Moreover, this temperature contrast introduces considerable asymmetry in important meteorological parameters.

The atmosphere can be heated in a variety of ways involving several complicated processes. When one considers only the dry atmosphere, most of the solar radiation will be absorbed at the earth surface, and the air parcels after receiving this energy in the form of sensible heat will become unstable and move vertically up (updrafts) in order to cool down. Thus, adiabatic ascent during daytime, when ground is hot, will act as a heat sink (cooling), while nighttime descent will act as a heat source for maintaining the temperature of lower layers as the ground cools. The diurnal variations are thus caused by vast differences of thermal effects of the surface. Chinese researchers (Yeh 1982) have noted important diurnal variations over the western Tibetan Plateau. Earlier studies (Flohn 1960; Koteswaram 1958) have also highlighted its importance as an elevated heat source for the establishment and maintenance of the summer monsoon. The interannual variability of heat sources has been observed to be large in the regions where the heating is strong (Pal et al. 1993).

However, the situation is different for the moist atmosphere. When radiatively active clouds are absent, the situation is initially same as that for the dry atmosphere. But if there is a moisture supply from the surroundings, moisture convergence into this region will give rise to clouding after parcels reach the lifting condensation level. In the unstable layers of the atmosphere the buoyancy of parcels will be maintained and deep convection can develop if moisture convergence continues in the region. Two things happen at this stage. First, due to precipitation over this region, the ground cools down, which will reduce the thermal contrast with the surrounding region. Second, the incoming solar radiation will be reflected back to space at the cloud tops, diminishing the supply of energy into the surface–atmospheric (or the ocean–atmosphere) column. This might result in an overall cooling (clouds heat the atmosphere and cool the surface) of the column, which could initiate more stable lapse rate conditions. In the course of time, the atmospheric column will again turn cloud free. Thus, clouds possess a strong autoregulatory mechanism.

Another scenario can also be constructed on the role of clouds during the monsoon period. Yasunari (1979) has noted two dominant modes, of around 40 and 15 days, in the summer monsoonal fluctuations after analyzing satellite cloudiness. In a later study, Sikka and Gadgil (1980) have shown two preferred locations of maximum cloud zones (MCZ): one over India (north of 15°N) and another (secondary) over the equatorial Indian Ocean. They have also found that the cloud bands have a strong tendency to move northward in all phases of a monsoon and could persist for a few days at a particular latitude. When a monsoon is active, warmer air ascends over monsoon land areas and relatively colder air descends over oceanic areas, which goes with an east–west circulation (Krishnamurti 1971). Like latent heat release, radiative forcing associated with clouds is another important diabatic process that drives

the circulation of the atmosphere. The clouds are generally categorized into three types: low, medium, and high (the ISCCP clouds are also classified into these categories). In fact, these clouds of different height categories affect radiation in different ways. The radiation can also affect clouds significantly. If one considers the presence of only one cloud type and its associated radiative effect in a surface–atmospheric column, then low clouds cool the column above, high clouds warm the column below, while middle clouds warm the column below and cool the column above the level where they are present (Paltridge and Platt 1976). Low clouds in practice radiate at the temperature of the underlying earth's surface, which results in strong cooling of overlaying atmospheric layers. Thus, interaction of longwave radiation with clouds may alter the thermal stratification of cloud layers through cloud-top cooling and cloud-base warming mechanism. Also, the presence of clouds may induce differential cooling between clear and cloudy regions. Hence, the longwave radiative process may increase convergence into the cloud system, which may, in turn, enhance precipitation at the surface in the cloudy regions.

With this background knowledge, it is now possible to perceive the variability induced by clouds in the monsoon rainfall due to their radiative effects only. Let us consider a situation during the active phase of the monsoon when the MCZ is located over India and the Indian Ocean region is initially cloud free. Then, if low clouds appear in the equatorial zone, they shall cool the column above and sinking motion of cold air over the adjacent cloud-covered ocean will increase. It could, in turn, strengthen the rising motion over India and, possibly, increase the quantum of rainfall there, too. In a similar situation, if high clouds cover the Indian Ocean, the quantum of monsoon rainfall over India will decrease in view of the arguments presented in the previous paragraph. But if convection grows over the equator, while the monsoon is still active over India (i.e., active convection at both the preferred locations of MCZ), a zone of downward motion will appear somewhere in between the equator and the position of MCZ over India. With the establishment of this zone of descending motion, the monsoon trough (a region of low pressure) has to adjust its position over the monsoon land areas. If it shifts northward then it will mark the beginning of break monsoon over India (Raghavan 1973; Dakshinamurti and Keshavamurty 1976). Thus, it is clearly expected from the above discussion that large variability can be introduced by the radiative effects of clouds. Moreover, it depends on cloud type and the location of cloud bands in the meridional direction. In other words, clouds can significantly influence the temperature contrast in the monsoon region affecting the external conditions and internal feedbacks discussed earlier by Meehl (1994a,b) in an attempt to explain the varying performance of monsoon from one year to another.

The design of the experiments for this study requires the radiative forcing of externally imposed clouds when SST forcing is also present. But, for specifying the observed clouds in the model, their optical properties—which directly influence their radiative effects—must be known a priori. We have used the ISCCP C1 datasets for this purpose. The ISCCP clouds have been taken because the data are as close to observations as possible and the optical properties of different categories of clouds are fairly accurate (Rossow et al. 1993). To our knowledge, no such study has been reported so far that has used ISCCP clouds (or the observed clouds) to examine the interannual variability of monsoons. This study therefore constitutes a first attempt in this direction using the ISCCP data in a more complete atmospheric general circulation model. It is important to point out here that the purpose of these experiments is not to express any judgment on the impact of ISCCP clouds on the model simulations of monsoon variability. It is rather to stress the importance of time-dependent cloudiness that is consistent with the model dynamics and to examine how a model responds if this condition is not satisfied. The study may, therefore, provide a new insight into the response of the model when the radiative feedbacks of clouds are considered together with the SST data.

The main aim of this study is twofold. On the one hand, it investigates how a GCM responds when observed clouds are specified externally over the Asian summer monsoon region and simulates the interannual variability of monsoon, while on the other hand, it examines the sensitivity of rainfall over India to initial conditions. A series of sensitivity experiments (120-day simulation runs) were performed with the atmospheric global model of the Laboratoire de Météorologie Dynamique (LMD GCM). The total number of such numerical experiments was eight; the first four experiments were performed with initial conditions of 1 May 1987, and the other four with that of 1 May 1988. In the next section, the important features of the LMD GCM and the derivation of cloud optical properties from ISCCP C1 data are briefly described. Next, the results of this study are presented with the help of 90-day mean (June–August) fields of precipitation, streamfunction, velocity potential, and circulation, and their differences from various experiments performed for this study. Although monsoon rainfall during the month of September contributes appreciably, in some years, to the seasonal total rainfall amounts in this region, it has not been considered here as the length of each simulation run is restricted to just 120 days. Finally, the main findings of this study are summarized in the last section.

2. Model and experimental design

We have used the LMD GCM for carrying out the sensitivity experiments to initial conditions, the SST forcing, and the radiative forcing of clouds. This section is devoted to the general description of the model that

has evolved over a period of time and to the description of the methodology to incorporate ISCCP clouds into this model. The first version of this model has been described by Sadourny and Laval (1984). This is a finite-difference general circulation model that uses Arakawa's C-type grid for discretization of operators, and the grid points are regularly spaced in longitude and sine of latitude. One of the important characteristics of this model is that it has enhanced meridional resolution in the Tropics resulting from the area-conserving meshes. The horizontal resolution adopted for this study has 96 points in longitude against 72 points in sine of latitude. The model uses normalized pressure ($\sigma = p/p_s$) as its vertical coordinate with 15 layers. The time integration scheme is a combination of explicit schemes (the basic time step of 15 min is split into one Euler-backward step followed by four leapfrog steps). Fourier filtering is applied to the longitudinal derivatives near the poles to ensure uniform and longer time steps. Lateral diffusion is modeled by a mixed bi-Laplacian in which the inner part acts on sigma coordinate and the outer parts on pressure coordinate.

The physics of the model is fairly complete except that the diurnal cycle is not included into this version. Diurnal cycle must be included while studying clouds and solar radiation sensitivities with climate models. But here we do not resolve anyway the diurnal cycle of the clouds over the monsoon area due to the absence of the Indian geostationary satellite (INSAT) data. Moreover, deep convection dominates the active monsoon periods and diurnal cycle may affect only low clouds, which are generally present over the adjacent ocean. The diurnal variation in convection over deep tropical oceans is again relatively weak. It is, therefore, expected that no significant error is introduced by neglecting the diurnal cycle in the model simulations. Physical parameterizations include solar radiation, longwave radiation, large-scale condensation, adjustment for small-scale convection, cumulus convection, and a prognostic equation for cloud water.

At the surface, eddy fluxes are calculated using a bulk method with drag coefficients varying with vertical gradient properties. The description of all the parameterizations of physical processes included in this model may be found in Le Treut et al. (1994). The hydrological exchanges between vegetation and atmosphere are computed using a scheme, called sechiba, that allows eight types of vegetation cover within a grid box (Ducoudré et al. 1993; Laval et al. 1996).

This sensitivity study uses primarily the prescribed cloud fields, which are chosen to be as realistic as possible. Hence, the observed cloud fields of 1987 and 1988 from the ISCCP data have been utilized. It is necessary to allocate the ISCCP cloud fractions to various model layers, but this cannot be done without some hypothesis. The cloud radiative properties in the model are calculated from the path of LWC. It is also necessary to derive this fundamental quantity from the ISCCP data. The scheme to obtain cloud cover and LWC is first presented here for the sake of completeness. It may be recalled that ISCCP C1 analysis provides information of 132 variables, such as cloud amount, cloud-top temperature, albedos, cloud optical depths, among others, every 3 h over a spatial resolution of 280 km^2. However, validation studies are required for these analyses. One such comparison of C1 cloud amounts with those derived from Advanced Very High Resolution Radiometer (AVHRR) images has been done by Weare (1992). The mean C1 cloudiness was found to be only 6% higher than that of AVHRR. The global patterns of cloud optical thickness with temperature have been reported by Tselioudis et al. (1992).

The ISCCP C1 analyses for May–August for the years 1987 and 1988 were utilized over a region between 30°S–30°N and 30°–120°E. This region practically covers the entire area of influence of the Asian summer monsoon. The ISCCP C1 data, however, do not contain information from the Indian geostationary satellite positioned in this region.

As a consequence, the analysis for this region relies entirely on the coverage by the passage of polar-orbiting satellites. The time resolution of the cloudiness is poorer. A composite field is first prepared for each day using the ISCCP data available at 0600, 0900, and 1200 UTC. These hours generally correspond to daytime hours over the monsoon region. From the composite data of each day, cumulated histograms of 5-day cloud statistics are produced that serve to determine mean cloud properties and are then interpolated to the model grid. Note that the technique of histogram partitioning used here allows the actual definition of averaged cloud fields, which is less meaningful when performed by direct averaging of these quantities. The histogram partitioning used for ISCCP divides the cloudiness by optical depth (five levels) and cloud-top pressure (seven levels). Each cloudy pixel thus belongs to one of the 35 categories depending on the optical depth and the top pressure of the cloud it represents (Fig 1). From the ISCCP classification, it is also possible that at a particular pressure level, clouds with different optical depths could be present. Since cloud cover is a key parameter in the model, it must be appropriately defined because any error in cloud cover will affect both shortwave and longwave radiative transfer calculations. For the experiments presented here, an effective cloud cover, C_f, has been first computed using cloud fractions at a given interval of cloud optical depth. Thus,

$$C_f = \sum_{i=1}^{5} C_i, \tag{1}$$

where C_i are cloud fractions at given intervals τ_i of cloud optical depth. The effective cloud optical depth is then computed as a weighted mean given by

$$\tau_f = \sum_{i=1}^{5} C_i \tau_i / C_f. \tag{2}$$

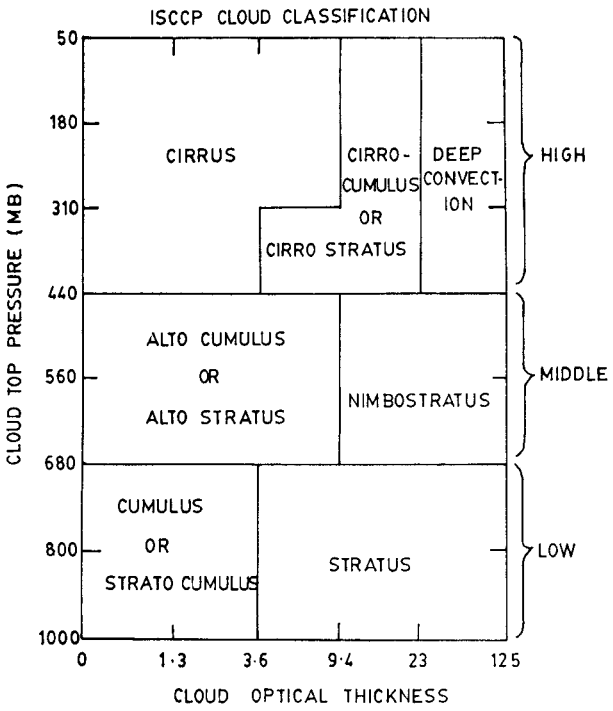

FIG. 1. Schematic ISCCP classification of clouds based on cloud optical thickness and cloud-top pressure.

In this manner, the effective cloud cover and effective cloud optical depth are computed at each ISCCP pressure level.

The LMD GCM includes a cloud prognostic scheme to take into account the cloud–radiation–water cycle interactions, where the cloud radiative properties are derived from the liquid water path (W, in grams per square meter) defined for each layer as

$$W = \int \rho l_{\text{cld}}\, dz, \tag{3}$$

where l_{cld} is the liquid water content equal to $q^{\text{cld}} - q_s(T)$ and ρ is the liquid water density. For longwave radiative transfer calculations, cloud emissivity is determined as

$$\epsilon = 1 - e^{-\kappa W}, \tag{4}$$

where the absorption coefficient κ is set equal to 0.13 $m^2\ g^{-1}$ for all cloud types (Stephens et al. 1990; Bony et al. 1992).

The shortwave cloud radiative properties are described by an asymmetry factor, a single scattering albedo, and a cloud optical thickness, τ. The asymmetry factor is set equal to 0.86 and 0.91 for the two 0.2–0.68-μm and 0.68–4.0-μm bands, respectively. The cloud optical thickness is defined in the model according to the Mie theory (Fouquart et al. 1990) as

$$\tau = \frac{3W}{2r_e}. \tag{5}$$

The effective radius (r_e) of particles is assumed to be 20 μm for water clouds and 40 μm for ice clouds. The radiative transfer calculations are performed for a plane parallel atmosphere assuming random overlap of clouds within the atmospheric column.

For the numerical experiments using ISCCP cloud parameters, we wish to deduce LWC consistently with (5). As we do not have the temperature inside the cloud, we have, however, chosen a mean value of the effective radius, $r_e = 30$ μm, in order to invert (5). This choice of the mean value of r_e tends to diminish a little the optical thickness of high clouds, when they are inserted back into the model, and tends to increase it for the low clouds. This feature tends to diminish one bias of the ISCCP data, which is to underestimate low cloudiness. Cloud amounts and LWC are then interpolated to the σ levels of the model. A hypothesis has been made here: the clouds are specified at the levels where their tops have been defined in the C1 climatology. In the absence of any kind of definite distribution, it is probably the easiest way to assign appropriate location to clouds, derived from ISCCP data, in atmospheric models. This ensures a reasonable radiation budget at the top of the atmosphere. The surface radiation budget may be more inaccurate and the profile of atmospheric absorption shifted toward higher levels.

The noticeable differences in the ISCCP clouds for 1987 and 1988 are seen in the mean condensed water content (CWC) of clouds in the monsoon region. This variable essentially represents the vertically integrated liquid water of clouds in an atmospheric column, obtained in the manner described above. The 5-day averages of cloud cover and cloud optical properties have been used, hence only the synoptic timescale variations of observed cloudiness are considered in the simulations. Using these pentads, one can also interpolate the cloud variables in time to give a smooth transition as the integrations progress. This has not been done here because the response of the circulation to radiative perturbation is not immediate, but takes a few days, and creates the desired smoothness in dynamical features. Instead of presenting all the pentad of CWC for the 4-month period, typically the mean CWC for the July months is shown in Fig. 2 for 1987 and 1988. In Fig. 2a, two zonal bands of CWC appear in the El Niño year 1987—one over India, and the other over the region south of the equator in the Indian Ocean. Also, the region around 10°N is practically cloud free and no contour of CWC from the Indian Ocean crosses this latitude. However, during the good monsoon year of 1988, CWC contours freely cross the 10°N latitude and the aforesaid zones of CWC coalesce into one covering the whole region (Fig. 2b), which shows an active summer monsoon during this period. Moreover, the distribution of CWC is very dense over India and it is mainly concentrated north of 10°S in the monsoon region. One can also note the low values of CWC south of 10°S in the Indian Ocean. Thus, the morphology of their distribu-

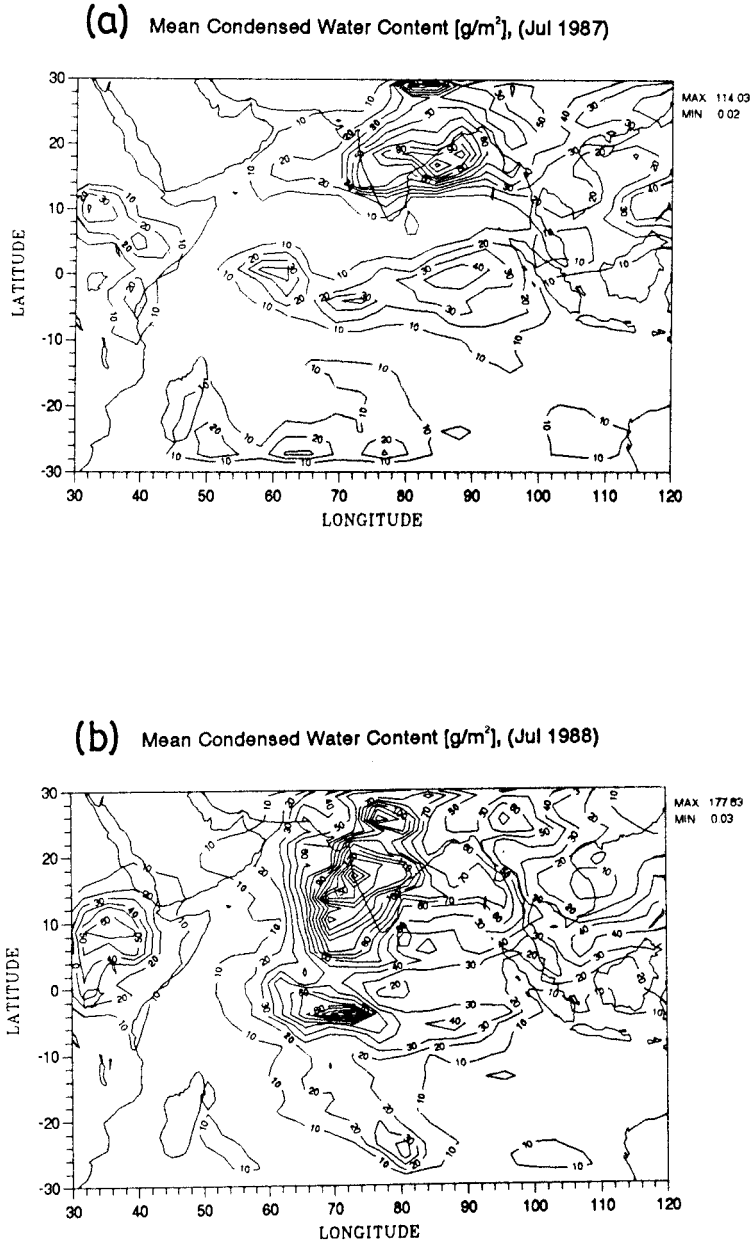

FIG. 2. Vertically integrated cloud water over the monsoon region (monthly averages) for July: (a) 1987, (b) 1988. Contour interval: 10 g m^{-2}.

tion in the two contrasting monsoons is very different. The maximum values of CWC corresponding to 1987 and 1988 also show marked differences, though their geographical locations are same during the two monsoons. For example, the July mean maximum value of CWC for 1987 is only 114.3 g m^{-2} (Fig. 2a), whereas for 1988 its value reaches 177.8 g m^{-2} (Fig. 2b). Indeed, the CWC computed using the relations (1)–(5) from the ISCCP data display the important features of the interannual variations in the region. Moreover, the average fields of CWC (pentads) can portray, in effect, the strength of convective activity during summer monsoon. Since the ISCCP climatology consists of a long series, some of the derived parameters can be utilized usefully to study both the intraseasonal and interannual variations of the important events in the Tropics where cloud feedbacks play an active role.

3. Results

Two sets of numerical experiments, each consisting of four simulations, were initialized with ECMWF analyses of 1 May 1987 and 1 May 1988, respectively, and were forced by the observed SSTs of 1987 and 1988

TABLE 1. List of numerical experiments.

Experiment	Initial conditions	SST	Clouds
I87-S87-CM	1 May 1987	1987	Model clouds
I87-S88-CM	1 May 1987	1988	Model clouds
I87-S87-C87	1 May 1987	1987	ISCCP clouds 1987
I87-S88-C88	1 May 1987	1988	ISCCP clouds 1988
I88-S87-CM	1 May 1988	1987	Model clouds
I88-S88-CM	1 May 1988	1988	Model clouds
I88-S87-C87	1 May 1988	1987	ISCCP clouds 1987
I88-S88-C88	1 May 1988	1988	ISCCP clouds 1988

for the period from May to August. These experiments (both control and sensitivity runs), of 120-day duration each, are summarized in Table 1. The first column in this table contains the abbreviations used for referring to a numerical experiment in the text. Thus, the abbreviation I87-S87-CM refers to the simulation that has been carried out with the initial conditions of 1 May 1987 (I87), sea surface temperatures that have been specified for 1987 (S87), and model clouds (CM) that are internally computed using the prognostic equation for cloud water. An experiment with above initial conditions and SST, but using the ISCCP clouds of 1987, say, will be referred to as I87-S87-C87 in the text. The other simulations can also be identified easily in this manner.

For each set of initial conditions, two integrations were forced by SST alone where cloud parameters were internally calculated by the model. The rest of the model runs were forced with a coherent combination of SST and ISCCP clouds for 1987 and 1988 (i.e., only the combinations S87-C87 and S88-C88 of SST and clouds are considered in these simulations). Mean fields were then computed by considering the last 90 days July–August (JJA) in each integration. However, the important features of this sensitivity study are discussed here by using such 90-day average fields of streamfunction, velocity potential, precipitation, and winds. The mean fields of streamfunction and velocity potential, as well as their differences, of 1987 and 1988, are presented over the whole globe, while precipitation fields and 850-hPa circulation are presented over a region 20°S–40°N, 20°W–130°E. The average fields on visual inspection also demonstrate the clear differences in precipitation, velocity potential, and circulation of the model integrations performed with realistic sea surface temperatures for the two monsoons. The model thus captures the interannual features of monsoon when forced with SST alone. This is in agreement with the conclusions of Palmer et al. (1992). However, the distinct features of various runs are better illustrated with the help of difference fields; hence, the various model runs have been compared in the light of differences of JJA mean fields of precipitation and other meteorological parameters of interest.

a. Difference fields: June–August

In this section, various simulation experiments are compared in order to discuss mainly the variability of a monsoon and its sensitivity to radiative forcing, and the impact of initial conditions. The comparison between I87-S87-CM and I88-S88-CM will show how the model simulates the interannual variations of a monsoon when model produces its own clouds as the integrations progress, whereas a comparison of I87-S87-C87 and I88-S88-C88 will show how the cloud–SST patterns affect the interannual variability when the clouds are externally prescribed and need not be associated with any precipitation. The sensitivity of model simulations to initial conditions, with SST and model generated or imposed clouds in the monsoon region, is investigated from the whole ensemble (shown in Table 1) of eight numerical experiments performed for this study.

1) PRECIPITATION

The 90-day mean precipitation for the four experiments performed with I87 and forced with SST and clouds of 1987 are shown in Fig. 3. It is evident from Fig. 3a that in experiment I87-S87-CM (i.e., initial conditions of 1 May 1987, SSTs of 1987, and model clouds), precipitation is absent in the central part and is mainly concentrated in the eastern part and the west coast of India. But precipitation increases, as shown by Fig. 3c, when the ISCCP clouds (I87-S87-C87) are specified. However, when the integration is forced by SSTs of 1988 (I87-S88-CM), precipitation increases over India with model clouds (Fig. 3b). As expected, when the ISCCP clouds of 1988 are imposed (I87-S88-C88), the radiative forcing has further increased the precipitation (Fig. 3d) over India. Thus, the initial conditions I87 are not as important as the SST and clouds. The model simulations, I88-S87-CM and I88-S88-CM, show increased precipitation over central India in comparison to that from the simulations I87-S87-CM and I87-S88-CM. Similar experiments were performed with initial conditions I88. On comparison, it appears that the initial signal in I88 was very strong relative to that in I87. Some spectacular changes have been noted in the rainfall over India in the two experiments I88-S87-C87 and I88-S88-C88. Surprisingly, with I88, the precipitation decreases (figures not shown) over parts of central India with S88 and C88. In the equatorial Indian ocean, a strong belt of precipitation has been simulated in some of the experiments where 1988 SSTs have been specified. Why does the model simulation degrade, with initial conditions I88, when observed clouds C88 are imposed together with SSTs of 1988? This may, however, be answered by the weaker monsoon circulation arising from the suppressed land–sea contrast in temperature. This point will be elaborated further in the next section. The distribution of precipitation in all the experiments can be compared with the climatology (JJA) of Jaeger

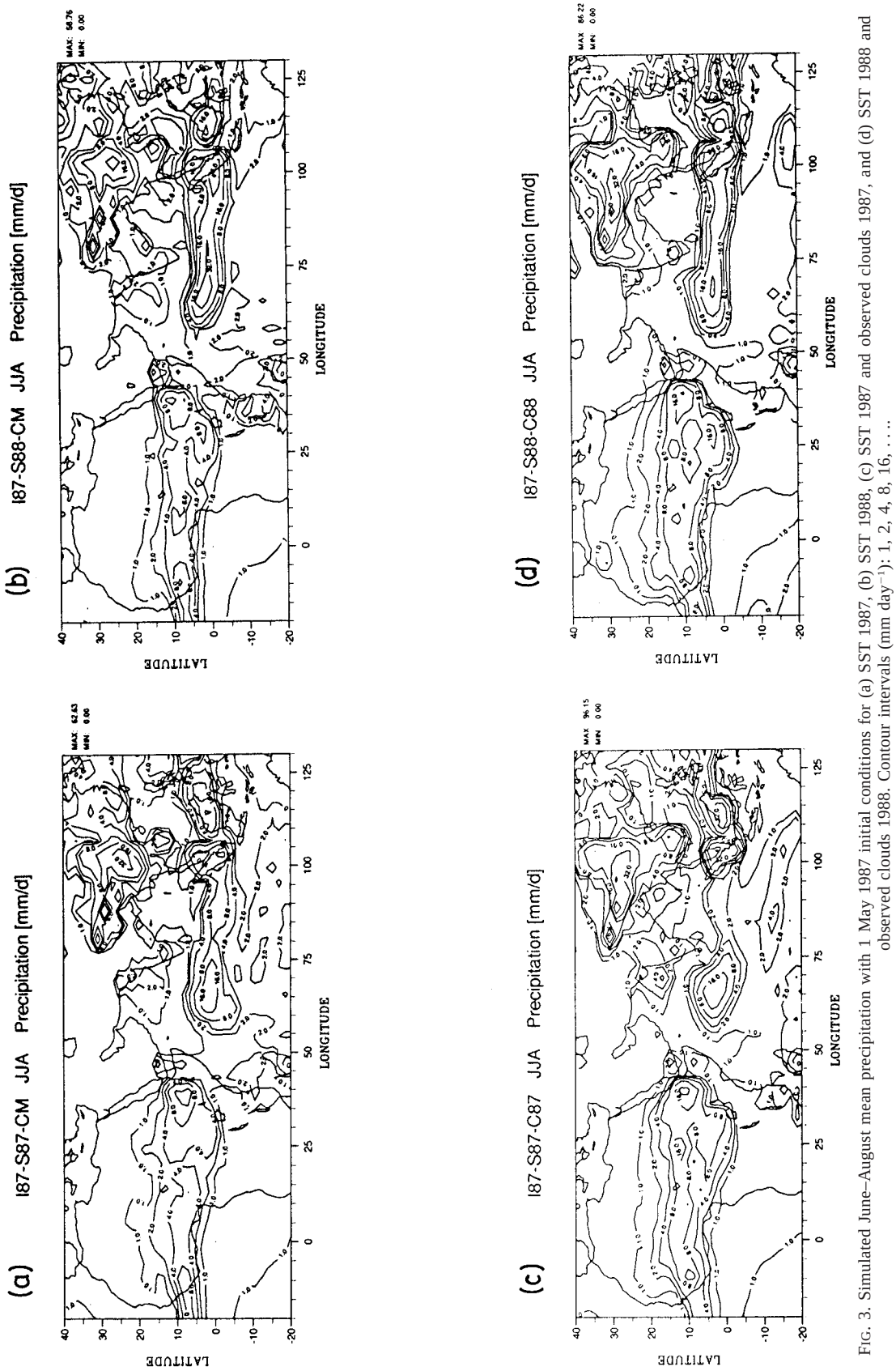

FIG. 3. Simulated June–August mean precipitation with 1 May 1987 initial conditions for (a) SST 1987, (b) SST 1988, (c) SST 1987 and observed clouds 1987, and (d) SST 1988 and observed clouds 1988. Contour intervals (mm day^{-1}): 1, 2, 4, 8, 16, . . .

(1976) and Legates and Willmott (1990). The important differences are mainly over the equatorial Indian ocean.

The differences of 90-day mean (JJA) precipitation of 1988 and 1987 are shown in Fig. 4, when forcings remain identical but only the initial conditions change. One can notice positive differences of precipitation (Fig. 4a) between I88-S87-CM and I87-S87-CM over India. This is also true for the simulations I88-S88-CM and I87-S88-CM (Fig. 4b). The differences over India, seen in Figs. 4a,b, are of interannual type (WCRP 1992), which may be expected as the signal in I88 is stronger. But the model obviously shows considerable sensitivity to initial conditions with dynamically evolving clouds during integrations. This kind of dependence of rainfall on initial conditions vanishes (Figs. 4c,d) over India, when the ISCCP clouds are imposed over the monsoon region. This means that large variability could be introduced in numerical simulations by the radiative forcing of clouds along with that arising from SST. This variability, hence cannot be explained by SST alone. It may be inferred from Fig. 4 that with both clouds and SST imposed the model simulation is less sensitive to initial conditions. This means that much of the uncertainty of predicting the month-to-seasonal variance of monsoon rainfall is linked to the clouds and the associated radiative forcing.

The interannual differences of precipitation are shown in Fig. 5. The precipitation differences (Fig. 5a) of simulation I88-S88-CM and I87-S87-CM resemble the analyzed station precipitation differences JJA 1988–1987 over India (WCRP 1992). However, the predicted differences are smaller in magnitude, by a factor of 2–4, than the analyzed station precipitation differences. Nevertheless, the model has demonstrated its ability to simulate reasonably well the interannual differences of 1988 and 1987 when cloud optical properties and other cloud parameters are computed by its cloud scheme. But, when ISCCP clouds are specified in the above model runs, one notices the positive differences in northern India and negative differences over the entire central part of India (Fig. 5b). That is, in I88-S88-C88 deficient rainfall is simulated in comparison to I87-S87-C87 in some parts of India. This implies degradation of model simulation I88-S88-C88 with observed clouds. It is indeed due to the response of the model to externally imposed cloudiness along with the SST data. However, in simulations with model-generated clouds, the response of the model is different when compared with the model response to imposed clouds though the SST data are identical in both the simulations. The precise reason for such a degraded simulation due to externally prescribed cloudiness will be explained with the help of the velocity differences. Yet it may be inferred from the above discussion that SST and clouds both affect the interannual variability.

2) 200-hPa streamfunction and velocity potential

Most of the variance of the mean motion is described by the rotational part of the circulation depicted by the streamfunction. During the Northern Hemisphere summer, the Tibetan high at 200 hPa is the most prominent feature of the upper-level circulation. The other climatological features seen in the summer mean flows are the mid-Pacific trough, the mid-Atlantic trough, and the tropical easterly jet over Asia and equatorial Africa (Krishnamurti 1971; Sadler 1975). The strength of the easterly jet and the lateral movements of the Tibetan anticyclone have important implications on the overall performance of monsoon in a particular year. However, the lateral movements of the Tibetan high in the upper atmosphere will not be addressed here.

For simulations carried out with initial conditions (I87) and sea surface temperatures (S87) of 1987, the mean streamfunction fields at 200 hPa are shown in Fig. 6. The streamfunction field corresponding to internally calculated clouds is presented in Fig. 6a and that corresponding to externally prescribed clouds (C87) from ISCCP data is shown in Fig. 6b. One can notice in both panels of Fig. 6 the most prominent, large anticyclone over the Tibetan highlands with an easterly flow over India. Also, a midlatitude trough over Hudson Bay in North America is clearly visible, though it is not located at its climatological position in the North Atlantic. A comparison of these panels further reveals that the anticyclonic circulation in the simulation I87-S87-C87 over Tibet has strengthened, relative to I87-S87-CM, with externally imposed clouds over the Asian summer monsoon region. Particularly, the zonal winds over India in Fig. 6b are stronger (as evidenced from the meridional gradient of streamlines) than those in Fig. 6a. This strengthening of the zonal winds (the easterly jet) in the upper troposphere over India is consistent with the increased precipitation (indicative of a stronger convective activity) in the simulation I87-S87-C87 (Fig. 3b) relative to I87-S87-CM (Fig. 3a). Since the differences of 200-hPa streamfunction fields of 1987 and 1988 model runs, both with and without externally specified clouds, are shown here, the maps showing 90-day mean streamfunction fields from the simulations performed with initial and boundary conditions of 1988 have not been included in the text.

The easterly jet over India in the upper troposphere is a very distinct feature of the summertime global circulation. How its characteristics vary in various runs can be inferred directly from the mean winds at 200 hPa (figures not shown). The jet is certainly weak (zonal winds of the order of 15 m s^{-1} in the simulation I87-S87-CM, but it is stronger in the simulation I87-S87-C87 as winds in excess of 20 m s^{-1} are noted there. The mean winds at 200 hPa from simulation I88-S88-CM show easterlies in excess of 20 m s^{-1} at 20°N reaching up to 15°E, which implies that the easterly jet has extended well into the African region. This does not happen in the sensitivity run I88-S88-C88, although the easterlies in excess of 20 m s^{-1} dominate the upper-air circulation over India. The easterly jet generally strengthens due to the intensification of the anticyclone,

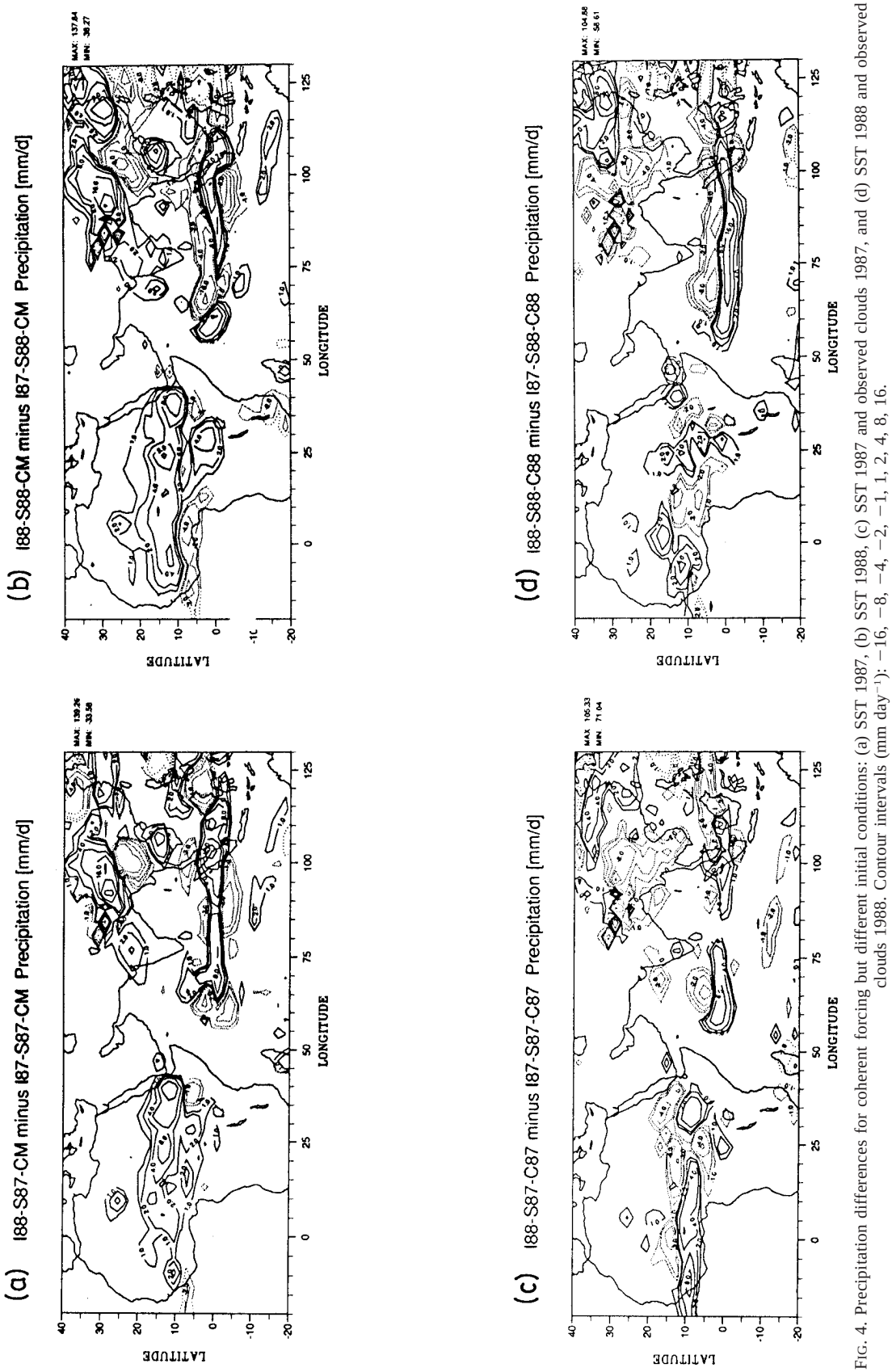

FIG. 4. Precipitation differences for coherent forcing but different initial conditions: (a) SST 1987, (b) SST 1988, (c) SST 1987 and observed clouds 1987, and (d) SST 1988 and observed clouds 1988. Contour intervals (mm day^{-1}): -16, -8, -4, -2, -1, 1, 2, 4, 8, 16.

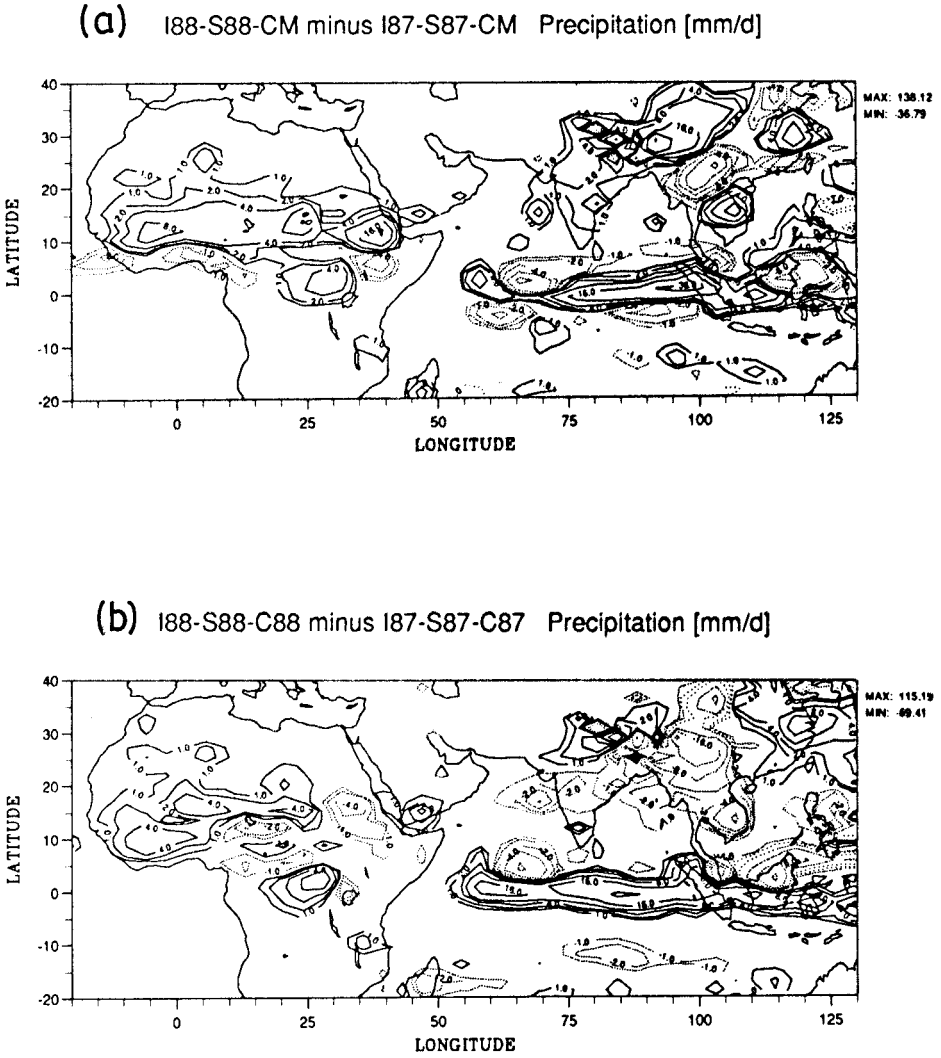

FIG. 5. Interannual variations of precipitation: (a) SST only, and (b) SST and observed clouds. Contour interval same as in Fig. 4.

which happens when the rainfall activity increases over India. The heating here then arises mainly due to the release of latent heat, which is controlled by the atmospheric dynamics. Therefore, on comparing the sensitivity run I88-S88-C88 with I88-S88-CM, it appears that the externally imposed clouds have adversely influenced the heating arising from the release of latent heat over the Indian subcontinent, while the reverse is true for the sensitivity run I87-S87-C87 with regard to I87-S87-CM.

The velocity potential field is generally used for depicting the divergent circulation on the global scale. It has a wavenumber 1 structure during summer months (JJA) with the divergence located over the warm waters near Indonesia in western Pacific and convergence over the Atlantic ocean. The 90-day mean (JJA) velocity potential fields from simulations performed with initial conditions I87 are shown in Fig. 7. The 200-hPa velocity potential field from I87-S87-CM (Fig. 7a) clearly shows the wavenumber 1 structure of the seasonal upper-level divergent circulation, with divergence over the western Pacific and convergence over the Atlantic Oceans. However, this seasonal large-scale structure is slightly modified in the Pacific Ocean due to the simulation of a dominant center of convection over Central America at 10°N, 80°W when external clouds (C87) are specified in the model run. Such a divergent center is present neither in the observations, nor in the simulation (I87-S87-CM) with model-generated clouds. In both of the above-mentioned simulations, the isopleths are parallel to longitude meridians over India, suggesting an east–west overturning there. Since an active monsoon is characterized by a strong east–west overturning (Krishnamurti 1971), the model has thus simulated a stronger monsoon with imposed clouds in I87-S87-C87 compared to that in the simulation I87-S87-CM. One can

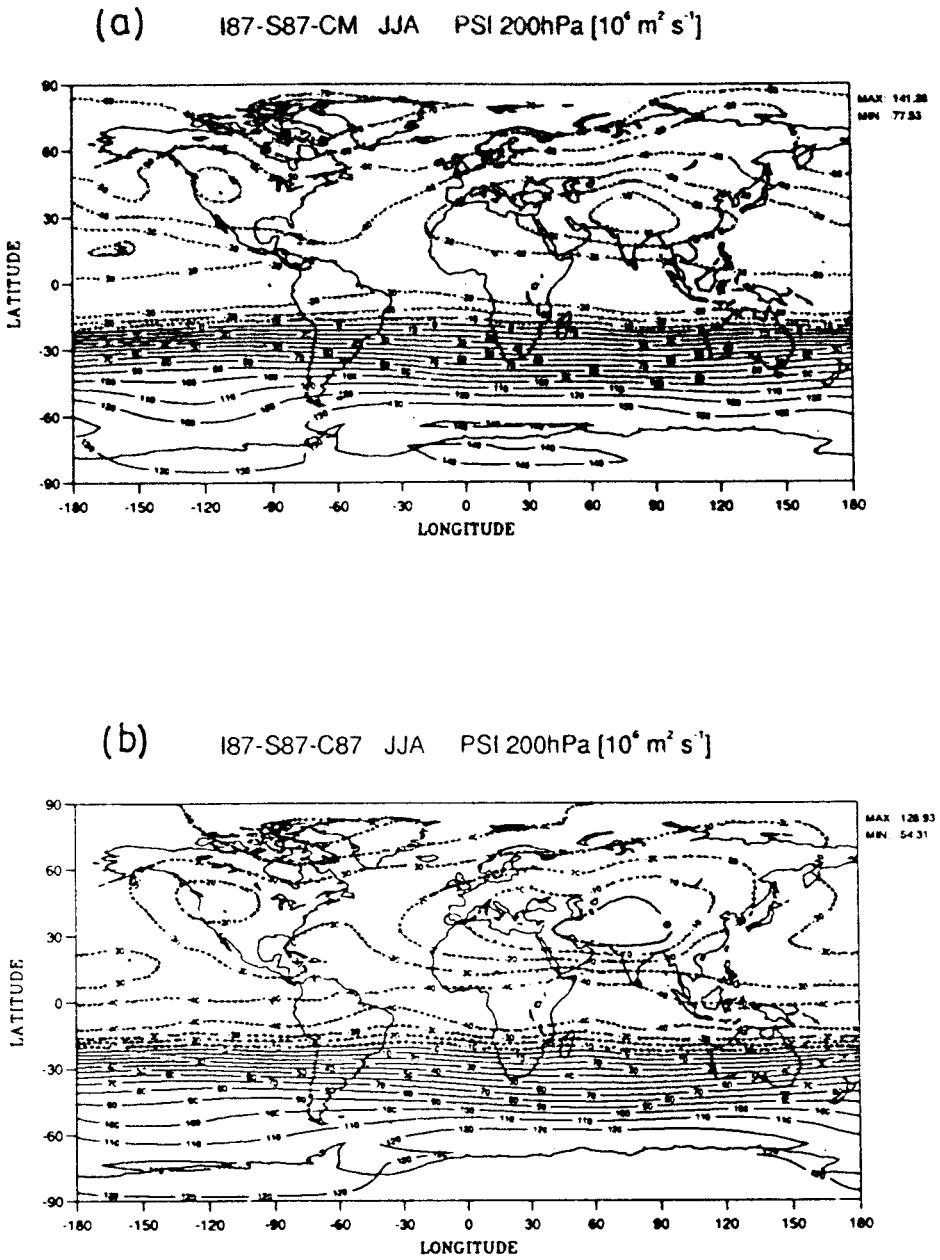

FIG. 6. Simulated JJA mean 200-hPa streamfunction with 1 May 1987 initial conditions for (a) SST 1987, and (b) SST 1987 and observed clouds 1987. Contour interval: 10 ($\times 10^6$ m^2 s^{-1}).

also notice in Fig. 7b a pronounced Walker circulation over the equator in the central Pacific ocean and a strong Hadley cell directed toward the Southern Hemisphere with the center of divergence located over the equator at 150°E. But such overturnings (zonal and meridional) in the Pacific Ocean are quite weak in the simulation I87-S87-CM (Fig. 7a) compared to those in I87-S87-C87 (Fig. 7b).

In the other set of model simulations performed with initial conditions I88, the wavenumber 1 structure of the divergence–convergence is almost maintained on the global scale when clouds are internally computed or prescribed from ISCCP data, along with SST of 1988. We do not reproduce the velocity potential maps for these simulations because their differences with respect to the corresponding simulations (with I87), along with the mean 200-hPa velocity potential maps, are shown here. The anomalous divergent center over Central America, noted above in I87-S87-C87, also appears in both of the simulations I88-S88-CM and I88-S88-C88. However, the main center of divergence in the Eastern Hemisphere, located over southeast China (28°N,

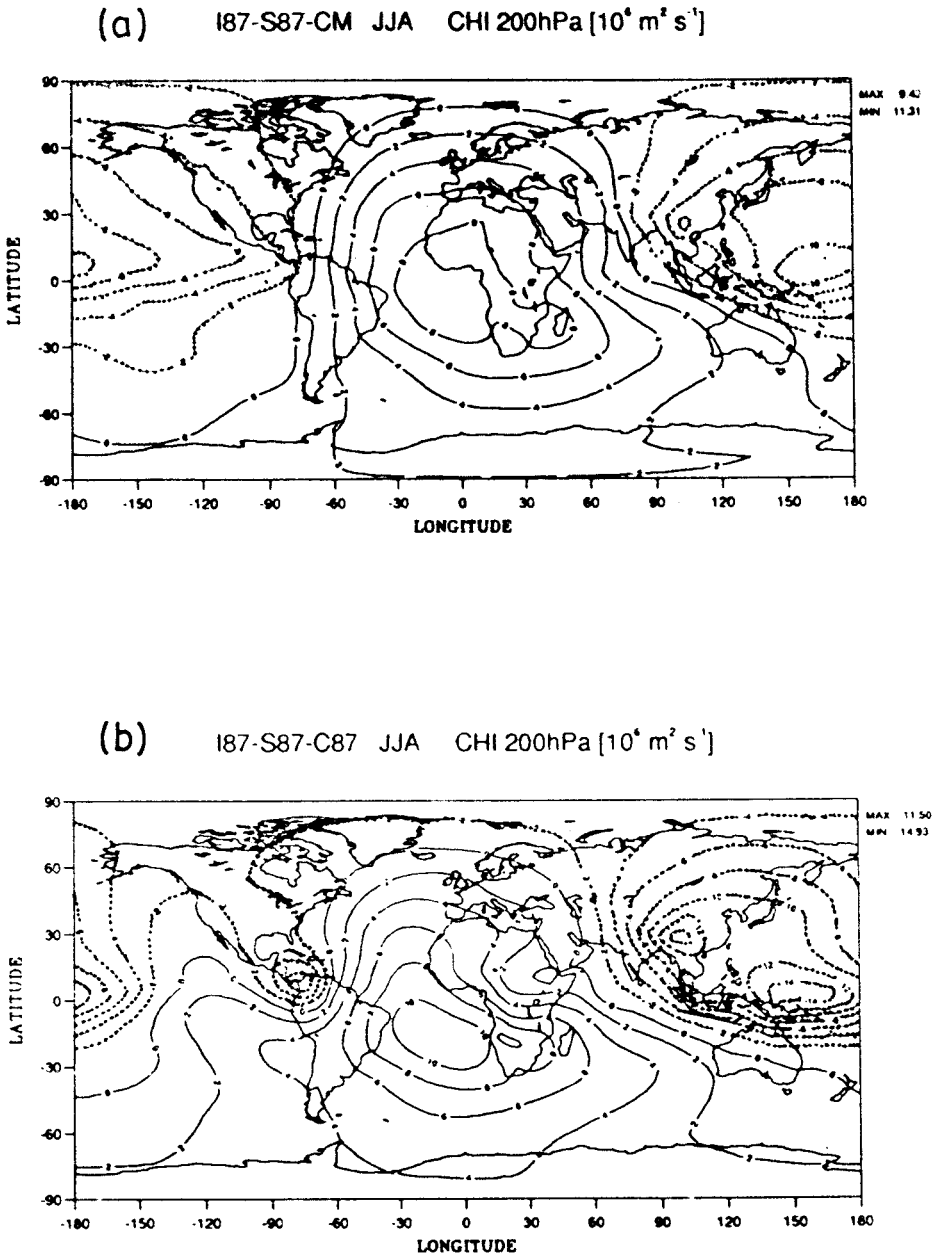

FIG. 7. Simulated JJA mean 200-hPa velocity potential with 1 May 1987 initial conditions for (a) SST 1987, and (b) SST 1987 and observed clouds 1987. Contour interval: 2 ($\times 10^6$ m^2 s^{-1}).

100°E), is displaced to the west of its climatological position in the western Pacific (Sperber et al. 1994). Another secondary divergence center is also simulated due to increased convective activity over East Africa. The upper-level divergent circulation in the simulations (I88-S88-CM and I88-S88-C88) shows pronounced east–west overturnings over India and in the central Pacific region, but the divergent center in I88-S88-CM is more intense than that seen in I88-S88-C88 (figures not shown). The monsoonal outflow center in both the simulations (I88-S88-CM and I88-S88-C88) extends to North Africa and exhibits strong Hadley type overturning over the Indian Ocean. This feature is present neither in I87-S87-CM, nor in I87-S87-C87. Thus, the radiative forcing due to clouds, which is modified by their optical properties, changes the orientation and gradients of isopleths of velocity potential and it could also broaden the longitudinal extent of divergent circulation to other areas of the monsoon region, influencing the weather over the region. Since the gradient of isopleths of 200-hPa velocity potential determine the strength of overturning (both Hadley and east–west type), the radiative

heating/cooling due to clouds could therefore introduce large variability, particularly in the monsoon region through such overturnings. Finally, it may be mentioned that the divergent center noted above over Central America also appears in the ECMWF model simulations reported by Sperber et al. (1994) while examining the sensitivity of the summer monsoon to horizontal resolution. However, it has a negligible effect on the stationary wave structure of the model since it does not extend beyond the tropical easterlies, as explained earlier by Boyle (1993).

The interannual differences of 200-hPa streamfunction and velocity potential fields are shown in Figs. 8 and 9, respectively. The 200-hPa streamfunction differences (Fig. 8a) between the simulations I88-S88-CM and I87-S87-CM, performed with model clouds, show a strong gradient between the equator and 30°N. This is indicative of a strong easterly flow over much of the Tropics except over the equatorial region of Pacific where a tropical westerly flow is associated with a pair of cyclones straddling the equator. Interestingly, when clouds are internally calculated, the model has been able to capture the relative increase in the strength of the easterly jet over Africa, a monsoon-related feature ob-

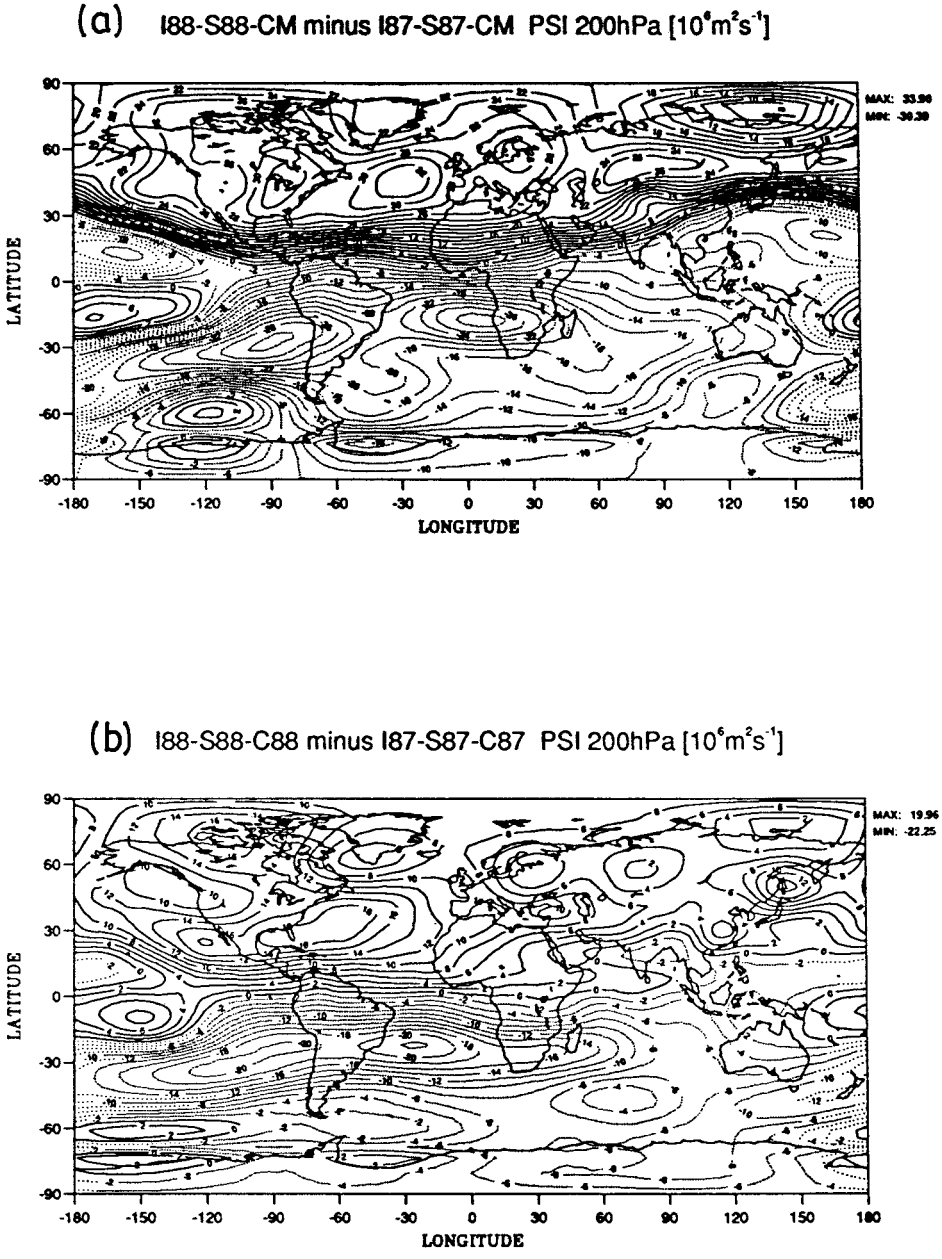

FIG. 8. Same as Fig. 5 but for 200-hPa streamfunction. Contour interval: 2 ($\times 10^6$ m^2 s^{-1}).

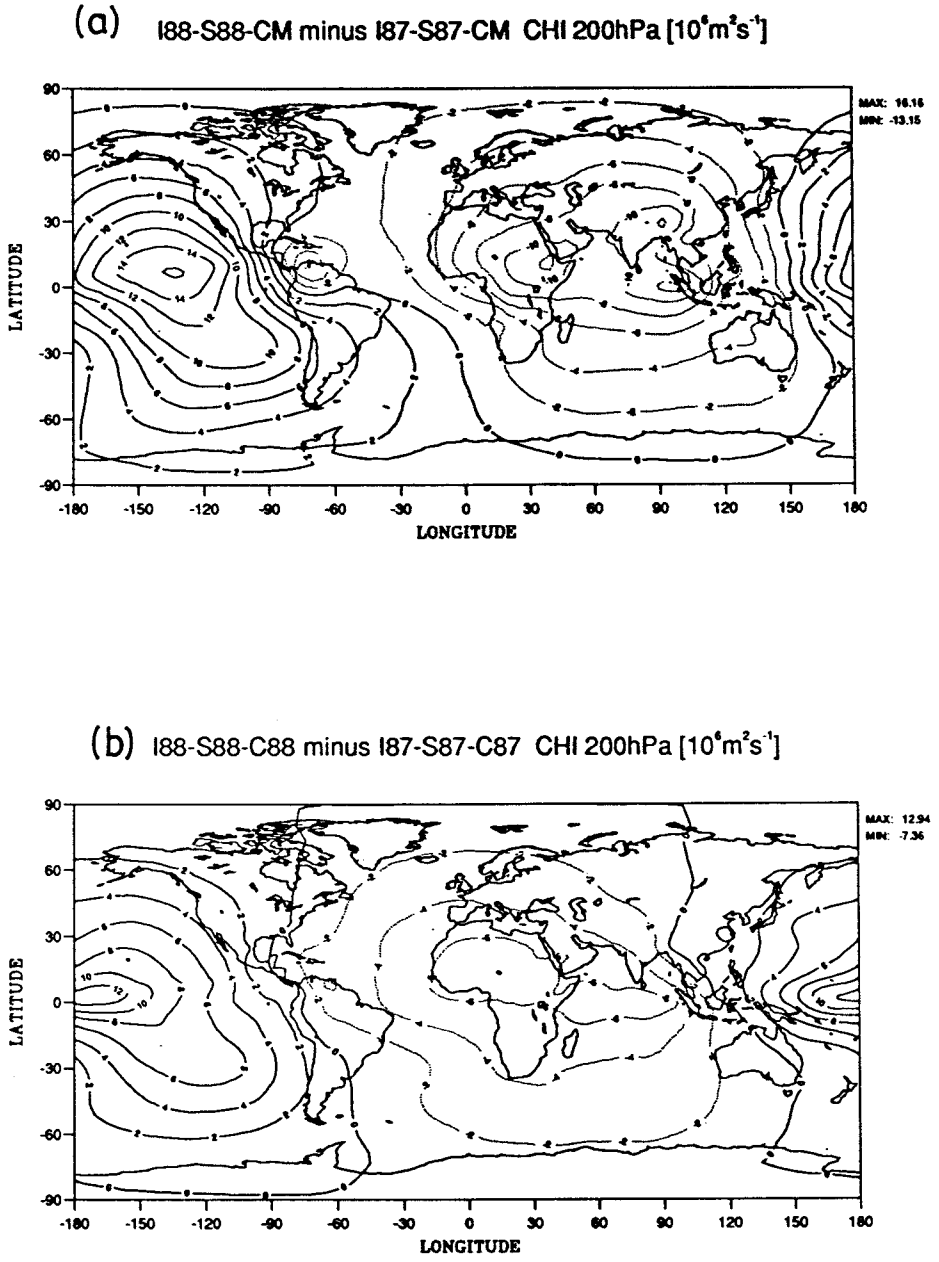

FIG. 9. Same as Fig. 5 but for 200-hPa velocity potential. Contour interval: 2 ($\times 10^6$ m^2 s^{-1}).

served in the ECMWF analyzed streamfunction differences (Palmer et al. 1992). The velocity potential differences (Fig. 9a) show a global-scale wavenumber 1 structure with a stronger convergence over eastern Pacific and a stronger divergence over the Indian Ocean except a small core of divergence over the equator at 60°W.

This is indicative of an above-normal summer monsoon over India during 1988 with model-generated clouds. However, when the ISCCP clouds are prescribed in the numerical simulations, both 200-hPa streamfunction and velocity potential differences show degradation in the simulated 1988 monsoon when they are compared with the ECMWF analysis differences of 1988 – 1987 (Palmer et al. 1992). Particularly, the streamfunction differences shown in Fig. 8a (with model clouds) are better over India and its vicinity than those shown in Fig. 8b (with imposed cloudiness). The streamfunction gradient between the equator and 30°N in Fig. 8b is rather weak, especially over the monsoon region. Moreover, the easterly flow over equatorial Africa has also weakened because of the appearance of a narrow zone of westerlies over east Africa extending up to south India. Also, it may be noted that the anomalous core of

divergence over Central America (Fig. 9a) has vanished in the 200-hPa velocity potential differences (Fig. 9b) computed from simulations I88-S88-C88 and 87-S87-C87. Thus, under the radiative forcing of prescribed clouds, the velocity potential difference field forms a wavenumber 1 structure showing divergence over monsoon region and convergence over the Pacific Ocean; nevertheless, the gradients of the isopleths in Fig. 9b have weakened relative to those in Fig. 9a. It may therefore be inferred from the above discussion that the response of the model to externally imposed cloudiness (over the monsoon region) deteriorates in the large-scale flow, relative to its response to dynamically consistent clouds.

3) 850-hPa wind

The streamfunction and velocity potential fields have clearly shown that radiative forcing of clouds has an important bearing on the monsoon circulation. We now examine its influence on the low-level circulation of this region. The onset of monsoon occurs with the establishment of the low-level cross-equatorial flow and the Somali jet over the Arabian sea. The Somali jet brings much-needed moisture over the Indian peninsula; therefore, its intensity directly affects the quantity of monsoon rainfall received by this region. The 850-hPa mean wind fields for the JJA period for the two simulations performed with the 1987 initial conditions (I87) have been shown in Fig. 10. The model has well reproduced the cross-equatorial flow and the Somali jet that characterize the monsoon circulation both with interactively computed clouds and with prescribed clouds. But the intensity of this low-level jet is weaker in I87-S87-CM than that simulated in I87-S87-C87. The cloud radiative properties of imposed clouds have thus induced an enhancement of the Somali jet in the latter simulation. This increase is possibly related to the thermal contrast between the Indian Ocean and the continent (the Indian landmass). It appears that the changes in the cloud radiative properties, besides increasing the convective activity over the monsoon region, have also increased the surface heating over India in the simulation I87-S87-C87 relative to I87-S87-CM, accentuating the thermal difference between the land and ocean. Such a pronounced meridional thermal gradient should be consistent with a relatively intense low-level jet over the Arabian sea in the experiment I87-S87-C87. In more specific terms, Fig. 10b shows wind speeds in excess of 10 m s^{-1} that occur over the entire Arabian sea region in association with strong easterlies (wind speeds exceeding 5 m s^{-1}) over the southern Indian Ocean and a broad cross-equatorial flow. Also note that the model has unrealistically simulated a strong southwesterly flow (wind speeds exceeding 15 m s^{-1}) at 850 hPa over northwest India. However, the aforementioned features of the low-level circulation are weaker (especially the Somali jet) in simulation I87-S87-CM (Fig. 10a) in comparison to those simulated in I87-S87-C87 (Fig. 10b). In another set of simulations (figures not shown) performed with the 1988 initial conditions (I88), the strength of the Somali jet (speed exceeding 10 m s^{-1} over the Arabian Sea) in I88-S88-CM is rather weak compared to the maximum velocity (>15 m s^{-1}) at the core of the observed jet in the 1988 JJA 850-hPa ECMWF analysis (WCRP 1992, p. 1.24). Nevertheless, the overall curvature of the cross-equatorial flow has been captured by the LMD model. However, when the ISCCP clouds are imposed together with SST in the experiment I88-S88-C88, slight weakening (speed less than 10 m s^{-1}) of the low-level jet has been noted over some parts of the Arabian Sea. It may therefore be inferred from the above discussion that the model response to externally imposed clouds together with SST has produced contrasting results: a better monsoon in the sensitivity run of 1987 (I87-S87-C87) than that of 1988 (I88-S88-C88). This point is further examined with the help of vector difference of the velocity fields from these two runs.

The vector wind difference field at 850 hPa, shown in Fig. 11, perhaps presents the most remarkable result of this sensitivity study. The interannual changes (1988 – 1987) in the ECMWF analysis (WCRP 1992, p. 2.4) show stronger equatorial easterlies over the Indian Ocean and an enhanced westerly inflow into western Africa. As can be seen from Fig. 11a, the wind differences show a stronger easterly flow north of 5°N, when the cloud radiative properties are internally calculated in the model. However, the difference flow is much weaker over the equator in comparison to the stronger easterly flow noted earlier in the ECMWF analysis differences. One can also notice stronger southwesterlies in Fig. 11a over the Arabian Sea and India. Though the observed and simulated difference fields disagree in the equatorial Indian Ocean, the vector wind differences at 850 hPa from the simulations I88-S88-CM and I87-S87-CM resemble those of the ECMWF 1988–87 analysis in the Arabian Sea. This shows that model has successfully simulated an intense southwest monsoon in 1988 in comparison to 1987 (WCRP 1992, p. 2.4). The stronger westerly inflow into West Africa can also be noted in Fig. 11a. But when ISCCP clouds are imposed over the monsoon region, the 850-hPa circulation shows dramatic changes. The difference field, shown in Fig. 11b, illustrates the interannual changes in the wind field resulting from the specification of observed clouds in simulations I88-S88-C88 and I87-S87-C87. Indeed, this figure shows that model has simulated a stronger monsoon in the sensitivity run I87-S87-C87 relative to I88-S88-C88. This is in contravention to reality, hence some explanation is warranted. We know that the monsoon arises as a result of land–sea temperature contrast. Therefore, a weaker Somali jet in I88-S88-C88 relative to I87-S87-C87 is consistent with the weaker thermal contrast caused by the imposition of observed cloud radiative properties, while the reverse is true in the simulation I87-S87-C87. The precise mechanism of this

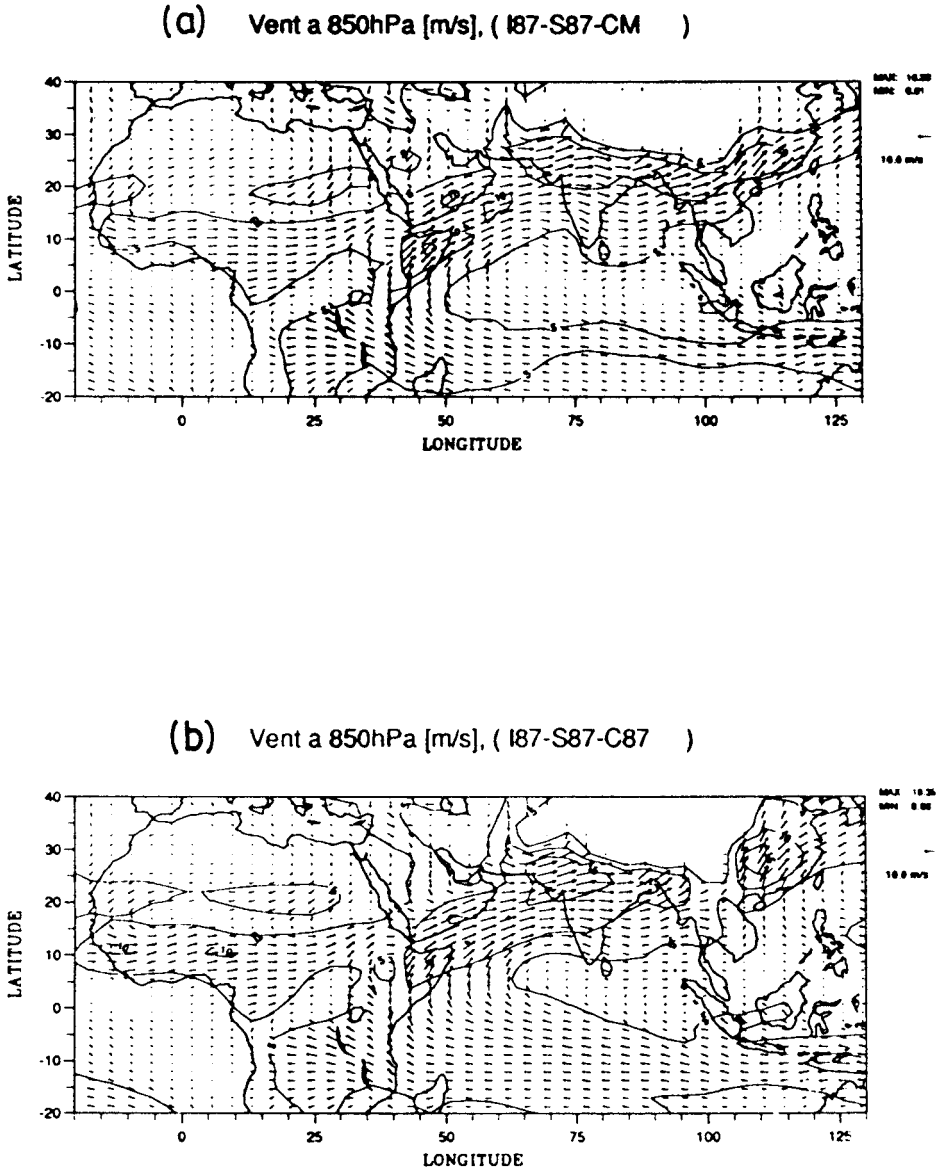

FIG. 10. Simulated June–August mean 850-hPa wind field with 1 May 1987 initial conditions for (a) SST 1987, and (b) SST 1987 and observed clouds 1987. Contour interval: 5 m s^{-1}.

weakening/strengthening of thermal contrast due to imposed clouds is elaborated in the next section. However, such a response of the model to observed clouds as externally imposed fields in a numerical simulation is interesting and suggests the need of a more sophisticated treatment of cloud microphysics in GCMs.

Some specific features of the vector difference field of winds at 850 hPa shown in Fig. 11b must be highlighted. In this figure, unlike Fig. 11a, a strong countermonsoon circulation over the summer monsoon region may be noticed in the lower atmosphere, along with a strong easterly flow over the Sahara. In the equatorial Indian Ocean, there appears a strong easterly flow to the east of 80°E and a westerly inflow to the west of this meridian. The westerly inflow from the Northern Hemisphere is more intense than that from the Southern Hemisphere. The structure of this low-level circulation over the Indian Ocean resembles Gill's solution, which represents the combined response of an analytical model of the tropical atmosphere to a symmetric heat source on the equator and an asymmetric heat source about the equator (Fig. 3; Gill 1980). Hence, when clouds are externally specified in the sensitivity run I88-S88-C88, an anomalous heat source develops on the equator with its center at 80°E in relation to the thermal contrast between land and ocean. In fact, this anomalous heat source arises due to weakening of the temperature contrast between the land and the sea caused by the local

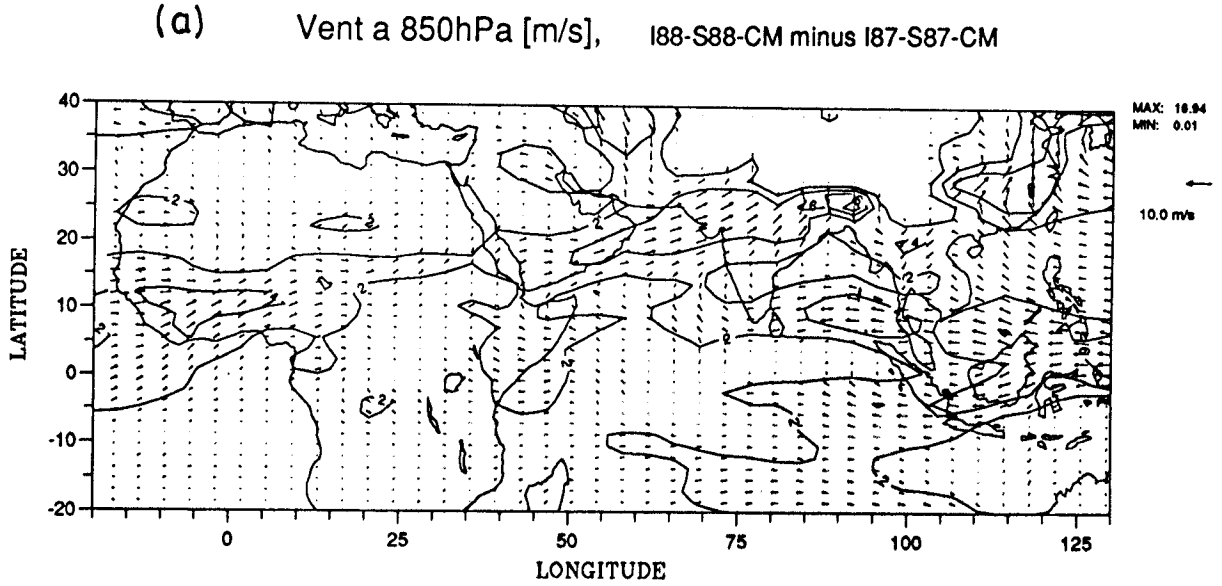

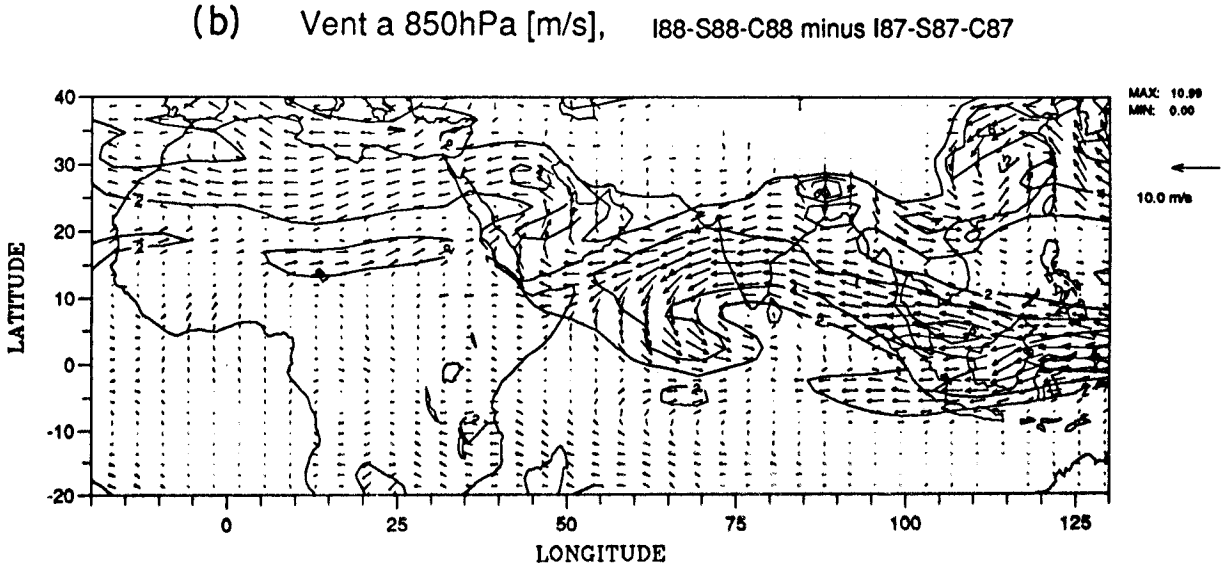

FIG. 11. Same as Fig. 5 but for 850-hPa winds. Contour interval: 2 m s^{-1}.

radiative effects resulting from the changed microphysical parameters (cloud drop radius, liquid water path, etc.) of the observed clouds. The excessive rainfall in the Indian Ocean at the equator in the precipitation difference (I88-S88-C88 minus I87-S87-C87), shown in Fig. 5b, is an evidence of this weakening in the land–sea temperature contrast due to radiative effects of the imposed clouds. In an observational study on summer monsoon of 1987 such a countermonsoon circulation was earlier discovered by Krishnamurti et al. (1989). This countermonsoon circulation at 850 hPa during 1987 precluded adequate supply of moisture over India. This is why 1987 was a bad monsoon year. In model simulations with imposed cloudiness, however, its presence in the difference field clearly implies that the model has simulated a weak monsoon with initial conditions and imposed forcings of 1988 compared to those of 1987.

b. All-India rainfall time series

The all-India rainfall was also computed by adding the daily rainfall at all the grid points in the Indian region. Figure 12 shows such time series of precipitation from the normal runs (SST and model clouds) and the sensitivity runs (SST and imposed clouds). The evolution of all-India rainfall shown in Fig. 12a (model clouds case) suggests the onset of monsoon on 1 June (the normal date of onset) in 1988 (thick line), whereas it is delayed by about a week in 1987 (dotted line). Moreover, based on rainfall amounts, the model has simulated a good monsoon in 1988, while 1987 clearly appears to be a weak monsoon year. When observed clouds are specified over the monsoon region, the evolution of daily rainfall from two simulations (Fig. 12b) also shows the impact of radiative forcing of externally imposed clouds on precipitation. The oscillations induced by the radiative forcing of prescribed clouds are clearly seen in the rainfall time series of simulations I88-S88-C88 (thick line) and I87-S87-C87 (dotted line). But the oscillations in the precipitation series from the sensitivity runs are stronger than those noted in the corresponding series from the simulations performed with dynamically consistent model clouds. It appears that fluctuations in the rainfall during a monsoon season may be closely associated with the radiative effects of clouds in this region. However, this inference needs to be substantiated with the help of more numerical experiments on the changed radiative properties of clouds.

4. Summary and conclusions

The interannual variability of summer monsoons has been studied with the help of the LMD GCM. Two sets of simulations were performed using the initial conditions prepared from the ECMWF analyses of 1 May 1987 and 1988 with observed sea surface temperatures. For some experiments the relevant cloud optical properties were derived from ISCCP data for the summer months of 1987 and 1988. The vertically integrated cloud water derived from ISCCP data provides clear differences in the two monsoon years. The typical July field, over the monsoon region in 1987, shows two well-separated bands where CWC contours are mainly concentrated, namely, one over India and other in the south Indian Ocean lying between the equator and 10°S. However, during 1988 such a separation in the CWC distribution is not noticeable. But the structure is essentially similar to that of 1987, as the two rainbands, depicted by two regimes of CWC maxima, are clearly visible in 1988 over the aforesaid regions (Fig. 2b), together with a minima in CWC near the equator. Also, it may be noted that the CWC amounts in 1988 are superior to those of 1987 and that their contours are mainly concentrated north of 10°S. Thus, there are important differences in the morphology of contours and their values in the two monsoon years. From the differences in CWC amounts of 1987 and 1988, it may be expected that the associated radiative effects due to clouds could introduce significant variability over the monsoon region. The assessment of this variability was one of the main aims of this study. For this purpose, the microphysical parameters were specified in some numerical simulations to obtain the response of the model to such externally imposed fields. For each set of initial conditions, two experiments were also performed where the cloud parameters were derived from cloud liquid water computed prognostically in the model. All numerical experiments carried out for this study were of 120-day duration. The mean fields were then computed using the last 90 days of the model integrations.

The 90-day mean fields (JJA) show considerable sensitivity to initial conditions when cloud optical properties are internally calculated in the model using the prognostic equation for liquid water. However, with both clouds and SST imposed, the model simulation is less sensitive to initial conditions. This is an important finding of this study. Furthermore, it also demonstrates that radiative forcing arising from clouds could introduce large variability in model simulations. The signature of this signal can be seen in the difference fields of precipitation and other meteorological parameters in the lower and upper atmosphere. The positive precipitation differences over northwest India and Africa show increased precipitation in 1988 when model generates its own clouds. The simulated precipitation differences resemble the observed rainfall differences 1988 – 1987 over India. Thus, the LMD GCM has been able to simulate successfully the interannual variations of summer monsoons with interactive clouds that are dynamically consistent with the dynamics and thermodynamics of the GCM. The 200-hPa streamfunction and velocity potential fields and the 850-hPa circulation (both mean and difference fields) corroborate the above result.

When optical properties of observed clouds are imposed in model runs, the interannual precipitation dif-

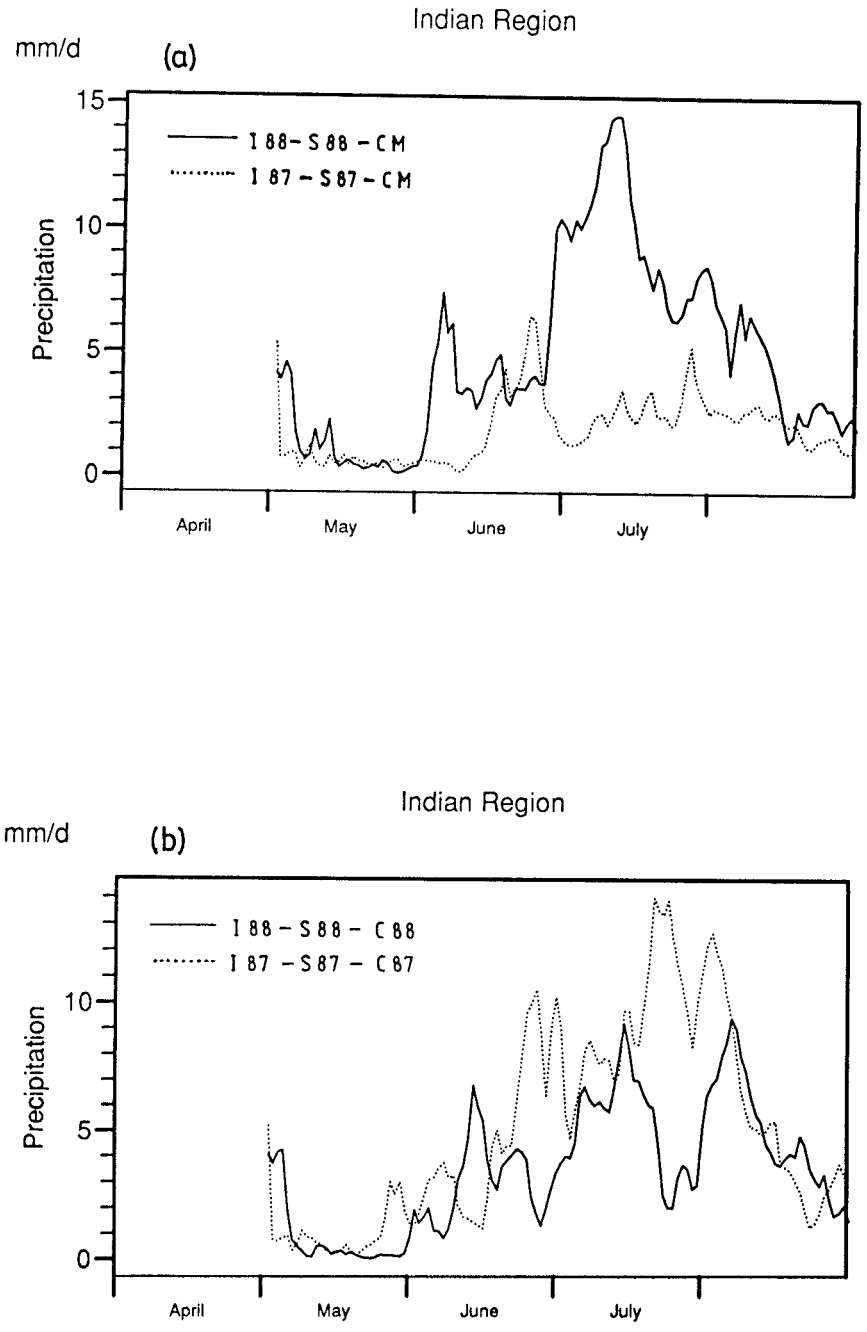

FIG. 12. Evolution of area-averaged precipitation over India: (a) I88-S88-CM, initial conditions 1 May 1988 and SST 1988 (thick line); I87-S87-CM, initial conditions 1 May 1987, and SST 1987 (dotted line). (b) I88-S88-C88: initial conditions 1 May 1988, SST 1988, and observed clouds 1988 (thick line); I87-S87-C87, initial conditions 1 May 1987, SST 1987, and observed clouds 1987 (dotted line). Units: mm day^{-1}.

ferences show some degradation in model-simulated rainfall. The reduced precipitation in the simulation I88-S88-C88 over central India in comparison to the corresponding model run for 1987 gives prominence to the variability introduced by cloud forcing. The precipitation differences are positive over northwest India and negative over central India. The negative precipitation differences in this region may be attributed to the strong countermonsoon circulation simulated by the model in 1988 relative to the 1987 simulation. Moreover, in the equatorial Indian Ocean there are easterlies in the region east to 80°E and a westerly inflow to the west of this meridian. The structure of this lower-atmospheric flow closely resembles the combined response of a linear

model of the atmosphere to a symmetric heat source on the equator and an asymmetric heat source about the equator (Gill 1980). It therefore suggests the presence of an anomalous heat source at the equator immediately below the Indian subcontinent in the model run I88-S88-C88.

What causes this equatorial heating in the Indian Ocean? An explanation in this regard should be in order. The equatorial heating is believed to be a consequence of the weaker land–sea temperature contrast caused by the imposition of the observed cloud properties. Normally clouds develop in response to the dynamical, thermal, and moisture state of the atmosphere, but in the ISCCP runs the cloud properties are imposed and need not be associated with any precipitation at all. In fact, the radiative response will be to suppress convection. We know that monsoon system is driven by land–sea temperature contrast. Therefore, the local response over land to the imposed cloud properties is the dominant influence for the incorrect simulation of rainfall and 850-hPa flow difference of 1988 relative to 1987 in the model runs with imposed cloudiness. Principally, in 1988 high concentration of CWC are present over the Indian monsoon land regions. This will serve to limit the heating of the land and give rise to weak land–sea contrast, a more stable atmosphere, and a weak Somali jet (borne out by Fig. 11b). As such, the ocean mode of the precipitation will be preferred. During 1987 the ISCCP CWC is much smaller than for 1988 over the subcontinent (Fig. 2) and as such has little influence on the land–sea temperature contrast with the I87-S87-C87 run being similar to the I87-S87-CM run. If the local effect is the cause, the 1987 ISCCP CWC should be consistent with (or even of lower concentration) than that produced in the I87-S87-CM run, and in 1988 the ISCCP CWC will be larger than for I88-S88-CM run.

The degradation in the model runs with prescribed clouds can also be seen in the streamfunction and velocity potential difference fields at 200 hPa when they are compared with the ECMWF analysis difference 1988–87. The streamfunction differences simulated by the LMD GCM with model clouds show better agreement with ECMWF analysis differences over India and its vicinity than the differences simulated with imposed cloudiness. Over the southern Indian latitudes, a narrow zone of westerlies at the upper level is noticed in the streamfunction difference field from the simulations I88-S88-C88 and I87-S87-C87. It is expected through the thermal wind relationship as a strong countermonsoon circulation exits in the lower levels. The existence of westerly (difference) flow implies weakening of the tropical easterly jet. Although the velocity potential difference field has a wavenumber 1 structure with divergence over the monsoon region and convergence over the Pacific, the zonal and meridional overturnings weaken when observed clouds are specified in the model runs. The evolution of all-India rainfall also shows degradation, illustrated by reduced precipitation over central India, in the simulation of the Indian summer monsoon circulation with imposed cloudiness.

In conclusion, the study reveals interesting effects of cloud-optical properties on the interannual variability of summer monsoons. These properties have been satisfactorily modeled in the LMD GCM. The main cause for the degradation seen in model simulations is the radiative heating due to the imposed clouds, which reduces the land–sea contrast in temperature. Moreover, this study emphasizes the importance of time-dependent cloudiness that is evolving in a consistent manner with the model dynamics and thermodynamics and provides new insights into the response of the model when the radiative feedbacks of clouds are considered together with the SST data. The most important results from this study are that 1) the cloud–SST patterns, together, affect the interannual variability, and (2) with both clouds and SST imposed the model simulation is less sensitive to initial conditions. Like the interannual variations, the other important variability of the monsoon system occurs at intraseasonal timescales. The abrupt cessation of rainfall over the plains of northern India causing breaks in the monsoon (Rao 1976), a regular phenomenon during July and August, is one such example. For a better understanding of monsoons, the role played by the radiative heating of clouds during the initiation of breaks in monsoon and it subsequent revival must also be examined with the sensitivity experiments using a GCM.

Acknowledgments. The authors wish to acknowledge Dr. Peter J. Lamb and the anonymous reviewers of this manuscript for their insightful comments and very useful suggestions, which greatly improved the quality of presentation. We also thank Drs. Katia Laval and Jan Polcher of LMD Paris and Dr. Harish Upadhyaya of IIT Delhi for helpful discussions. One of us (OPS) would like to acknowledge Dr. V. Ramanathan of Scripps Institute of Oceanography for helpful discussions and Dr. Girija Jayaraman of IIT Delhi for going through the final manuscript. This research was supported by the Indo-French Centre for the Promotion of Advanced Research/Centre Franco-Indien pour la Promotion de la Recherche Avancée, New Delhi, under Contract 711-1.

REFERENCES

Atlas, R., N. Wolfson, and J. Terry, 1993: The effect of SST and soil moisture anomalies on GLA model simulations of the 1988 U.S. summer drought. *J. Climate,* **6,** 2034–2048.

Bony, S., H. Le Treut, J.-P. Duvel, and R. S. Kandel, 1992: Satellite validation of GCM simulated annual cycle of earth radiation budget and cloud forcing. *J. Geophys. Res.,* **97,** 18 061–18 081.

Boyle, J. S., 1993: Sensitivity of dynamical quantities to horizontal resolution for a climate simulation using the ECMWF (cycle 33) model. *J. Climate,* **6,** 796–815.

Charney, J., and J. Shukla, 1981: Predictability of monsoons. *Monsoon Dynamics,* J. Lighthill and R. P. Pearce, Eds., Cambridge University Press, 99–109.

——, W. J. Quirk, S.-H. Chow, and J. Kornfield, 1977: A comparative

study of effects of albedo change on drought in semi-arid regions. *J. Atmos. Sci.,* **34,** 1366–1385.
Chen, T.-C., and M.-C. Yen, 1994: Interannual variation of the Indian monsoon simulated by the NCAR Community Climate Model: Effect of the tropical Pacific SST. *J. Climate,* **7,** 1403–1415.
Dakshinamurti, J., and R. N. Keshavamurty, 1976: An oscillation of period about one month in the Indian summer monsoon. *Indian J. Meteor. Geophys.,* **27,** 201–203.
Das, S. N., M. R. M. Rao, and N. C. Biswas, 1988: Monsoon season (June–September 1987). *Mausam,* **39,** 325–340.
——, D. S. Desai, and N. C. Biswas, 1989: Monsoon season (June–September 1988). *Mausam,* **40,** 351–364.
Ducoudré, N., K. Laval, and A. Perrier, 1993: SECHIBA, a new set of parameterizations of the hydrologic exchanges at the land–atmosphere interface within the LMD atmospheric general circulation model. *J. Climate,* **6,** 248–273.
Flohn, H., 1960: Recent investigations on the mechanism of the ''summer monsoon'' of the southern and eastern Asia. *Monsoons of the World,* S. Basu et al., Eds., Hind Union Press, 75–88.
Fouquart, Y., J. C. Buriez, M. Herman, and R. S. Kandel, 1990: The influence of clouds on radiation: A climate modeling perspective. *Rev. Geophys.,* **28,** 145–166.
Gill, A., 1980: Some simple solutions of heat-induced tropical circulation. *Quart. J. Roy. Meteor. Soc.,* **106,** 447–462.
Hou, A. Y., and R. S. Lindzen, 1992: The influence of concentrated heating on Hadley circulation. *J. Atmos. Sci.,* **49,** 1233–1241.
Jaeger, L., 1976: Monatskarten des Niederschlages für die ganze Erde. *Ber. Dtsch. Wetterdienstes,* **139,** 1–38.
Koteswaram, P., 1958: Easterly jet stream in the tropics. *Tellus,* **10,** 407–410.
Krishnamurti, T. N., 1971: Observational study of the tropical upper tropospheric motion field during the Northern Hemisphere summer. *J. Appl. Meteor.,* **10,** 1066–1096.
——, H. S. Bedi, and M. Subramaniam, 1989: The summer monsoon of 1987. *J. Climate,* **2,** 321–340.
——, ——, and ——, 1990: The summer monsoon of 1988. *Meteor. Atmos. Phys.,* **42,** 19–37.
Laval, K., R. Raghava, R. Sadourny, and M. Forichon, 1996: Simulations of the 1987 and 1988 Indian monsoons using the LMD GCM. *J. Climate,* **9,** 3357–3372.
Legates, D. R., and C. J. Willmott, 1990: Mean seasonal and spatial variability in gauge-corrected, global precipitation. *Int. J. Climatol.,* **10,** 111–127.
Le Treut, H., Z. X. Li, and M. Forichon, 1994: Sensitivity of the LMD General Circulation Model to greenhouse forcing associated with two different cloud water parameterizations. *J. Climate,* **7,** 1827–1841.
Lindzen, R. S., and A. Y. Hou, 1988: Hadley circulations for zonally averaged heating centered off the equator. *J. Atmos. Sci,* **45,** 2416–2427.
Madden, R. A., and P. R. Julian, 1994: Observations of 40–50-day tropical oscillations—A review. *Mon. Wea. Rev.,* **122,** 814–836.
Meehl, G. A., 1994a: Influence of the land surface in the Asian summer monsoon: External conditions versus internal feedbacks. *J. Climate,* **7,** 1033–1049.
——, 1994b: Coupled land–ocean–atmosphere processes and south Asian monsoon variability. *Science,* **226,** 263–267.
Pal, P. K., A. Kasahara, and A. P. Mizzi, 1993: Interannual variability in circulations and energetics of a climate model over Asian summer monsoon region. Tech. Rep. ISRO-SAC-TR-99-93, Indian Space Research Organisation, Bangalore, India, 48 pp. [Available from Publications and Public Relations Unit, ISRO Headquarters, Antariksh Bhavan, New BEL Road, Bangalore 560 027, India.]
Palmer, T. N., C. Branković, F. Molteni, and S. Tibaldi, 1990: Extended range predictions with ECMWF models: Interannual variability in operational model integrations. *Quart. J. Roy. Meteor. Soc.,* **116,** 799–834.
——, ——, P. Viterbo, and M. J. Miller, 1992: Modeling interannual variations of monsoons. *J. Climate,* **5,** 399–417.
Paltridge, G. W., and C. M. R. Platt, 1976: *Radiative Processes in Meteorology and Climatology.* Elsevier, 318 pp.
Raghavan, K., 1973: Break-monsoon over India. *Mon. Wea. Rev.,* **101,** 33–43.
Rao, Y. P., 1976: Southwest monsoon. *Synoptic Meteorology, Meteor. Monogr.,* No. 1, India Meteor. Dept., 1–367.
Rossow, W. B., and R. A. Schiffer, 1991: ISCCP cloud data products. *Bull. Amer. Meteor. Soc.,* **72,** 2–20.
——, A. W. Walker, and L. C. Garder, 1993: Comparison of ISCCP and other cloud amounts. *J. Climate,* **6,** 2394–2418.
Sadler, J. C., 1975: The upper tropospheric circulation over the global tropics. UHMET-75-05, University of Hawaii, Honolulu, HI, 35 pp. [Available from Dept. of Meteorology, University of Hawaii at Manoa, Honolulu, HI 96822.]
Sadourny, R., and K. Laval, 1984: January and July performances of LMD general circulation model. *New Perspectives in Climate Modeling,* A. Berger, Ed., Elsevier, 173–198.
Shukla, J., 1981: Dynamical predictability of monthly means. *J. Atmos. Sci.,* **38,** 2547–2572.
Sikka, D. R., and S. Gadgil, 1980: On the maximum cloud zone and the ITCZ over Indian longitudes during the southwest monsoon. *Mon. Wea. Rev.,* **108,** 1840–1853.
Sperber, K. R., and T. N. Palmer, 1996: Interannual tropical rainfall variability in general circulation model simulations associated with the Atmospheric Model Intercomparison Project. *J. Climate,* **9,** 2727–2750.
——, S. Hameed, G. L. Potter, and J. S. Boyle, 1994: Simulation of the northern summer monsoon in the ECMWF model: Sensitivity to horizontal resolution. *Mon. Wea. Rev.,* **122,** 2461–2481.
Stephens, G. L., S. Tsay, P. W. Stackhouse, and P. J. Flatau, 1990: The relevance of microphysical and radiative properties of cirrus clouds on climate and climate feedbacks. *J. Atmos. Sci.,* **47,** 1742–1753.
Tselioudis, G., W. B. Rossow, and D. Rind, 1992: Global patterns of cloud optical thickness variation with temperature. *J. Climate,* **5,** 1484–1495.
WCRP, 1992: Simulation of interannual and intraseasonal monsoon variability. WCRP-68, WMP/TD-470, WCRP, Geneva, Switzerland, 231 pp. [Available from Joint Planning Staff for WCRP, c/o World Meteorological Organization, Case Postale No. 2300, CH-1211 Geneva 20, Switzerland.]
——, 1993: Simulation and prediction of monsoons, recent results. WCRP-80, WMP/TD-546, WCRP, Geneva, Switzerland, 82 pp. [Available from Joint Planning Staff for WCRP, c/o World Meteorological Organization, Case Postale No. 2300, CH-1211 Geneva 20, Switzerland.]
Weare, B. C., 1992: A comparison of ISCCP C1 cloud amounts with those derived from high resolution AVHRR images. *Int. J. Remote Sens.,* **13,** 1965–1980.
Yasunari, T., 1979: Cloudiness fluctuations associated with the Northern Hemisphere summer monsoon. *J. Meteor. Soc. Japan,* **57,** 227–242.
Yeh, T.-C., 1982: Some aspect of thermal influences of Quinghai-Tibetan Plateau on the atmospheric circulation. *Arch. Meteor. Geophys. Bioklimatol.,* **31A,** 205–220.
Zhang, Z., and T. N. Krishnamurti, 1996: A generalization of Gill's heat-induced tropical circulation. *J. Atmos. Sci.,* **53,** 1045–1052.